Acta Pharmaceutica Sinica B 2024;14(10):4378–4395

Chinese Pharmaceutical Association
Institute of Materia Medica, Chinese Academy of Medical Sciences

Acta Pharmaceutica Sinica B

www.elsevier.com/locate/apsb
www.sciencedirect.com

ORIGINAL ARTICLE

PKCα inhibitors promote breast cancer immune evasion by maintaining PD-L1 stability

Jiaojiao Yu[a,b,†], Yujin Xiang[a,b,†], Yuzhen Gao[a,b], Shan Chang[c], Ren Kong[c], Xiaoxi Lv[a,b], Jinmei Yu[a,b], Yunjie Jin[a,b], Chenxi Li[a,b], Yiran Ma[a,b], Zhenhe Wang[a,b], Jichao Zhou[a,b], Hongyu Yuan[a,b], Shuang Shang[a,b], Fang Hua[a,b], Xiaowei Zhang[a,b], Bing Cui[a,b,*], Pingping Li[a,b,*]

[a]*State Key Laboratory of Bioactive Substance and Function of Natural Medicines, Institute of Materia Medica, Chinese Academy of Medical Sciences & Peking Union Medical College, Beijing 100050, China*
[b]*CAMS Key Laboratory of Molecular Mechanism and Target Discovery of Metabolic Disorder and Tumorigenesis, Chinese Academy of Medical Sciences & Peking Union Medical College, Beijing 100050, China*
[c]*Institute of Bioinformatics and Medical Engineering, School of Electrical and Information Engineering, Jiangsu University of Technology, Changzhou 213001, China*

Received 1 March 2024; received in revised form 20 June 2024; accepted 15 July 2024

KEY WORDS

Protein kinase C;
PD-L1;
β-TRCP;
Degradation;
Immune evasion;
Immunotherapy;
Combination strategies;
Breast cancer

Abstract Protein kinase C α (PKCα) regulates diverse biological functions of cancer cells and is a promising therapeutic target. However, clinical trials of PKC-targeted therapies have not yielded satisfactory results. Recent studies have also indicated a tumor-suppressive role of PKCs *via* unclear molecular mechanisms. In this study, we found that PKCα inhibition enhances $CD8^+$ T-cell-mediated tumor evasion and abolishes antitumor activity in immunocompetent mice. We further identified PKCα as a critical regulator of programmed cell death-ligand 1 (PD-L1) and found that it enhances T-cell-dependent antitumor immunity in breast cancer by interacting with PD-L1 and suppressing PD-L1 expression. We demonstrated that PKCα-mediated PD-L1 phosphorylation promotes PD-L1 degradation through β transducin repeat-containing protein. Notably, the efficacy of PKCα inhibitors was intensified by synergizing with anti-PD-L1 mAb therapy to boost antitumor T-cell immunity *in vivo*. Clinical analysis revealed that PKCα expression is positively correlated with T-cell function and the interferon-gamma signature in patients with breast cancer. This study demonstrated the antitumor capability of PKCα, identified

*Corresponding authors.
E-mail addresses: cuibing@imm.ac.cn (Bing Cui), lipp@imm.ac.cn (Pingping Li).
[†]These authors made equal contributions to this work.
Peer review under the responsibility of Chinese Pharmaceutical Association and Institute of Materia Medica, Chinese Academy of Medical Sciences.

https://doi.org/10.1016/j.apsb.2024.08.003

potential therapeutic strategies to avoid tumor evasion *via* PKC-targeted therapies, and provided a proof of concept for targeting PKCα in combination with anti-PD-L1 mAb therapy as a potential therapeutic approach against breast cancer, especially TNBC.

1. Introduction

Protein kinase C (PKC) is a calcium- and phospholipid-dependent serine/threonine-protein kinase that regulates intracellular signal transduction and contributes to cell proliferation, differentiation, apoptosis, and invasion[1]. The extended protein kinase C (PKC) family comprises the classical PKC (cPKC; PKCα, PKCβ, and PKCγ), atypical PKC (aPKC; PKCζ and PKCλ/ι), novel PKC (nPKC; PKCδ, PKCε, PKCη, and PKCθ) and PKN subfamilies[1,2]. PKC, a receptor for tumor-promoting phorbol esters, has long been considered an oncogene and potential therapeutic target for cancer therapy[1]. PKC activation modulates cell proliferation and survival by activating several intracellular signaling pathways, such as the MAPK/ERK pathway and the PI3K/AKT pathway[3-7]. Protein kinase C alpha (PKCα), encoded by *PRKCA*, is a member of the classical PKC family and plays pivotal roles in breast cancer proliferation, metastasis, stemness, and drug resistance[8,9]. In the immune system, PKCs also act as signal transduction mediators and are involved in innate and adaptive immunity[10]. Several small-molecule inhibitors or specific antisense oligonucleotides targeting PKCα and its family members have been developed and evaluated in clinical trials for patients with various types of cancer. However, the efficacy of these treatments is unsatisfactory[11]. Recently, a few studies have also demonstrated the tumor-suppressive role of PKC, but the details of the contradictory functions of PKC have not been determined[12,13]. Understanding the intrinsic characteristics of PKCs, especially from an immune system perspective, might help clarify the controversial issues regarding PKC function and the lack of efficacy of PKC-targeted cancer therapeutics[14].

Immune evasion is a hallmark of cancer and represents a major obstacle to effective therapeutic strategies[15,16]. Solid tumors, including breast cancer, are highly infiltrated with immunosuppressive immune cells, including regulatory T cells, myeloid-derived suppressive cells, tumor-associated macrophages, neutrophils, and dendritic cells, which contribute to $CD8^+$ T-cell exhaustion and tumor progression[17]. Immune checkpoint blockade (ICB) therapies targeting the programmed cell death-1 (PD-1) pathway or cytotoxic T lymphocyte antigen 4 have achieved unprecedented success against cancer by reactivating and boosting T-cell responses[18]. Antibodies against PD-1 (anti-PD-1) or programmed cell death ligand-1 (anti-PD-L1) are the most widely used ICB antibodies in the clinic for treating different tumors, including metastatic melanoma, non-small cell lung cancer, head and neck squamous cell carcinoma and triple-negative breast cancer (TNBC)[19-21]. However, compared to patients with melanoma, non-small cell lung cancer, and head and neck squamous cell carcinoma, the clinical response rate of ICB in breast cancer patients is relatively limited[22]. Due to the higher mutational load, immunogenic TNBC is amenable to immunotherapeutic intervention and has a greater response rate to ICB than ER^+ and $HER2^+$ breast cancer[23,24]. While ICB monotherapies have shown limited efficacy in TNBC patients, the treatment efficacy depends on the therapeutic setting, treatment line, and combination of immunotherapies with other anticancer drugs[25,26]. Current therapeutic options, such as chemotherapy or targeted agents with ICB, are only at the tip of the iceberg. The translation of experimental targeted therapeutic agents and combination therapeutic strategies with ICB into clinical benefits is still a welcome and ongoing challenge[25,27]. Understanding the basic biology of immune evasion in breast cancer is imperative for evaluating and developing new ICB combination strategies to prevent cancer progression.

PD-L1, a well-known immune evasion checkpoint, is widely expressed in various types of cancer cells and immune cells[28]. The expression of PD-L1 is positively correlated with the outcome of anti-PD-1/PD-L1 therapies. Consequently, PD-L1 serves as a predictive biomarker for the clinical response to anti-PD-1/PD-L1 mAbs[22,28,29]. Recent studies have shown that protein kinases play a critical role in regulating the protein quality control of PD-L1[2,30-32]. For example, glycogen synthase kinase 3β induces $PD\text{-}L1^{T180}$ and $PD\text{-}L1^{S184}$ phosphorylation and promotes β transducin repeat-containing protein (β-TRCP)-mediated PD-L1 degradation[33]. Janus kinase 1 induces $PD\text{-}L1^{Y112}$ phosphorylation, enhances PD-L1 glycosylation, and maintains PD-L1 stability[34]. Adenosine 5′-monophosphate -activated protein kinase dampens PD-L1 expression by triggering $PD\text{-}L1^{S195}$ or $PD\text{-}L1^{S283}$ phosphorylation[35,36]. Several protein kinases, including cyclin-dependent kinase 4 and hepatocyte growth factor receptor, can destabilize PD-L1 through other indirect pathways[37,38]. Characterization of the crosstalk between protein kinases and PD-L1 quality control may improve the understanding of the therapeutic efficacy of kinase inhibitors for cancer treatment, reveal regulatory networks related to PD-L1 expression, and provide new approaches for improving ICB efficacy. Indeed, many efforts have been devoted to discovering the synergistic effects of existing kinase inhibitors with ICB in cancer treatment[39].

In this study, we focused on the efficacy of PKCα inhibitors in cancer treatment and the role of PKCα in mediating the T-cell response in breast cancer. We postulated that PKCα is involved in tumor evasion and indeed showed that PKCα can act as a negative regulator of PD-L1 and promote $CD8^+$ T-cell-mediated anticancer immunity in breast cancer. Targeting PKCα in combination with anti-PD-L1 mAb therapy is a potential therapeutic approach for treating breast cancer, especially TNBC.

2. Methods

2.1. Cell culture

The breast cancer cell lines MDA-MB-231, MDA-MB-468, BT549 and the human embryonic kidney cell line HEK293T were obtained

from the National Infrastructure of Cell Line Resources, Peking Union Medical College (Beijing, China). 4T1 cells were provided by Dr. Bo Huang from the Institute of Basic Medicine, Chinese Academy of Medical Sciences & Peking Union Medical College. MDA-MB-231, MDA-MB-468, BT549, and 4T1 cells were cultured in DMEM supplemented with 10% FBS. HEK293T cells were cultured in IMDM supplemented with 10% FBS. All cells were maintained at 37 °C in a humidified atmosphere with 5% CO_2. Cell lines were routinely tested for potential mycoplasma contamination using commercial mycoplasma detection kits (Lonza, LT07-418). All tests were negative.

2.2. Reagents and antibodies

Cycloheximide, collagenase IV, and DNA I were purchased from Sigma−Aldrich (St. Louis, MO, USA). Go6976, Go6850, Ro-32-0432, bafilomycin A1, and MG132 were purchased from Selleck Chemicals (Houston, TX, USA). Enzastaurin and a PKCθ inhibitor (compound 20) were purchased from Aladdin (Shanghai, China). VigoFect transfection reagent was purchased from Vigorous Biotechnology (Beijing, China). Lipofectamine RNAiMAX transfection reagent and Lipofectamine LTX Reagent with PLUS Reagent were purchased from Thermo Fisher Scientific (Waltham, MA, USA). BCA protein quantitative kits were purchased from Applygen Technologies (Beijing, China). CCK-8 kits were purchased from Dojindo Laboratories (Kumamoto, Japan). A phosphoserine/threonine rabbit polyclonal antibody was purchased from Beyotime Biotechnology (Shanghai, China). Anti-PD-L1 (13684S), and anti-PKCα (59754S) antibodies were purchased from Cell Signaling Technology (Beverly, MA, USA). Anti-PKCα (ab57415), anti-PD-L1 (ab213480), and anti-phosphoserine (ab7851) antibodies were purchased from Abcam (Cambridge, MA, USA). Anti-PKCβ (12919-1-AP) and anti-PKCγ (14364-1-AP), anti-PD-L2 (18251-1-AP), anti-B7H3 (14453-1-AP), anti-PVR (27486-1-AP), anti-PVR (31447-1-AP), anti-Galectin9 (17938-1-AP), anti-CD86 (13395-1-AP), and anti-FGL1 (16000-1-AP) antibodies were purchased from Proteintech Group (Wuhan, China). Antibodies against HA, Myc, DDK, and GFP were purchased from MBL Beijing Biotech (Beijing, China). GAPDH and HRP-labeled secondary antibodies were obtained from ZSGB-Bio (Beijing, China). Alexa Fluor 488-, 594- or 647-conjugated secondary antibodies were purchased from Life Technologies (Carlsbad, CA, USA). Anti-mouse PD-L1 (clone 10F.9G2; catalog number BE0101), anti-mouse CD8α (clone YTS169.4; catalog number BE0117), and anti-IgG2b (clone LTF-2; catalog number BE0090) were obtained from BioXcell (Lebanon, NH, USA). The human CD274/PD-L1 CRISPR Plasmid and an anti-p-Thr antibody (sc-81526) were purchased from Santa Cruz (Dallas, TX, USA).

2.3. Plasmids

PD-L1-HA, PD-L1-Myc, β-TRCP-DDK, PKCα-DDK, PKCη-Myc, and PKCθ-Myc plasmids were purchased from Sino Biological, Inc. (Beijing, China). GFP-tagged PD-L1 and its truncations, PD-L1-ECD and PD-L1-ICD, were inserted into the PEGFP-C1 vector by standard subcloning. PD-L1 mutants (S80A and S184A) were generated using the Fast Mutagenesis System (TransGen Biotech, Beijing, China).

2.4. Gene set enrichment analysis (GSEA)

The TCGA BRCA database (dataset ID: TCGA.BRCA.sample Map/HiSeqV2, version 2017-10-13, $n = 1218$), TCGA LUNG database (dataset ID:TCGA.LUNG.sampleMap/HiSeqV2_PANCAN, version 2017-09-08, $n = 1129$), TCGA COAD database (dataset ID: TCGA.COAD.sampleMap/HiSeqV2_PANCAN, version 2017-10-13, $n = 329$), and pancreatic cancer dataset (dataset ID: TCGA.PAAD.sampleMap/HiSeaV2_PANCAN, version 2017-10-13, $n = 183$) were downloaded from the UCSC Xena. Among the cancer samples, the upper tenth (which was positively correlated with *PKC*) had the highest level of PKC expression. In contrast, the lower tenth (which was negatively correlated with *PKC*) had the lowest level of PKC expression. Using the signal-to-noise measure in the GSEA, we ranked 20,530 genes according to their association with the breast cancer groups (patients with *PKC* positively correlated vs. patients with *PKC* negatively correlated). Gene sets for heatmap presentation and GSEA were obtained from MSigDB. GSEA was conducted using MSigDB v6.1. The gene set was considered significant when the false discovery rate (FDR) was less than 0.25.

2.5. Generation of stably expressing cell lines

To generate cells stably expressing control-shRNA or *PKC*α-shRNA1/2, cells were infected with control or *PKC*α-shRNA1/2 lentiviral particles. Stable transfectants were selected in media supplemented with puromycin (Life Technologies) or by GFP cell sorting. After 2 to 3 passages in the presence of puromycin, the cultured cells were used for experiments without cloning. To establish cells stably expressing control or *PKC*α plasmids, empty vector or *PKC*α-*DDK* plasmids were transfected into cells with Lipofectamine LTX Reagent and PLUS Reagent according to the manufacturer's instructions. After 48 h of transfection, stable transfectants were selected in a medium supplemented with hygromycin for 14 days. After 2 to 3 passages in the presence of hygromycin, the cultured cells were used for experiments without cloning.

2.6. RNA interference

RNA interference was performed using Invitrogen™ Lipofectamine™ RNAiMAX Transfection Reagent following the manufacturer's instructions. The RNA interference primers used were as follows: si-m-*Prkca*_1, GGACGACTCGGAATGACTT; si-m-*Prkca*_2, GCAAAGGACTTATGACCAA; si-h-*PRKCA*_1, GGAAACAACCTTCCAACAACC; si-h-*PRKCA*_ 2, TAACACC ACCTGATCAGCTGGTTAT; si-h-*PRKCB*_1, GGAGTCCTG CTGTATGAAA; si-h-*PRKCB*_2, GCGACCTCATGTATCACAT; si-h-*PRKCG*_1, GCCTGTATTTCGTGATGGA; si-h-*PRKCG*_2, CCTACCGACCATGTTCAAT; si-h-β-*TRCP*_1, AAGTGGAAT TTGTGGAACATC; si-h-β-*TRCP*_2, ACAGGATCATCGGAT TCCA.

2.7. Quantitative real-time PCR

Total RNA was extracted using an RNA-Quick purification kit (Shanghai Yishan Biotechnology Co., Ltd., ES-RN001) following the manufacturer's instructions. The reverse transcription of the total cellular RNA was carried out using oligo (dT) primers and M-MLV reverse transcriptase (Promega, Madison, USA). According to the manufacturer's instructions, qPCR was performed using the KAPA SYBR FAST qPCR Master Mix (2 ×) Kit (Kappa Biosystem, USA). The following qPCR primers were used: *CD274* forward, 5′-TGCCGACTACAAGCGAATTACTG-

3′; *CD274* reverse, 5′-CTGCTTGTCCAGATGACTTCGG-3′; *PRKCA* forward, 5′-GCCTATGGCGTCCTGTTGTATG-3′; *PRKCA* reverse, 5′-GAAACAGCCTCCTTGGACAAGG-3′; *GAPDH* forward, 5′-GTCTCCTCTGACTTCAACAGCG-3′; and *GAPDH* reverse, 5′-ACCACCCTGTTGCTGTAGCCAA-3′.

2.8. Immunoblotting

The cells were collected and lysed on ice in RIPA lysis buffer (Beyotime Biotechnology, Shanghai, China) for 30 min. After centrifugation, the supernatants were collected, and the protein concentration was determined *via* a BCA protein quantitative kit. The homogenate supernatants were resolved by SDS−PAGE, and the proteins were subsequently transferred to PVDF membranes for immunoblot analysis. Signals were detected by a Tanon 5200 chemiluminescent imaging system (Tanon, Shanghai, China).

2.9. Immunoprecipitation and mass spectrometry (MS)

The cells were lysed in Co-IP lysis buffer (25 mmol/L Tris−HCl, 150 mmol/L NaCl, 2.5 mmol/L $MgCl_2$, 0.5% NP-40, 1 mmol/L EDTA, 5% glycerol) on ice for 30 min and centrifuged at 12,000 rpm for 30 min to remove debris. The cleared lysates were incubated with the indicated antibodies and Protein A/G Plus-Agarose (Santa Cruz Biotechnology, TX, USA) at 4 °C overnight. After washing, the immunocomplex was boiled in 2 × SDS sample buffer for 5 min. The samples were subjected to SDS-PAGE and immunoblotting. For mass spectrometry analysis, the samples were separated on SDS-PAGE gel followed by silver staining. The bands were extracted from the gel and subjected to LC−MS/MS sequencing and data analysis by QLBio Biotechnology Co., Ltd. (Beijing, China).

2.10. Immunofluorescence and immunohistochemistry

For immunofluorescence staining, cells or tissue sections were fixed in 4% paraformaldehyde at room temperature for 20 min, permeabilized in 0.5% Triton X-100 for 15 min, blocked with 3% bovine serum albumin for 15 min, and then stained with specific primary antibodies followed by corresponding secondary antibodies. Nuclei were stained with DAPI. After mounting, the cells were visualized using a confocal fluorescence microscope (Olympus, CA, USA). A human breast cancer microarray (HBreD050Bc01) was purchased from Shanghai Outdo Biotech Co., Ltd. for multiple immunohistochemistry. According to the manufacturer's protocol, the paraffin-embedded tissue sections were stained using a six-color labeled kit (TSA-RM) (PANOVUE Biotechnology Co., Ltd.). Briefly, the tissue sections were deparaffinized in xylene and hydrated in water through a graded alcohol series. After antigen retrieval with Trilogy buffer, the tissue sections were blocked with PBS plus 4% bovine serum albumin and 0.1% Triton X-100 at room temperature for 30 min. The tissue sections were stained with the indicated primary and corresponding secondary antibodies and incubated in the amplification diluent for 10 min. Primary antibodies were added for separate staining, and between the intervals of each staining, the antigen was re-treated with 10 mmol/L citric acid (pH 6.0) in a microwave oven. After extensive washing, the sections were incubated with DAPI solution and mounted using Prolong Diamond medium. Images were detected and captured using a confocal fluorescence microscope (Olympus, CA, USA).

2.11. Protein degradation inhibition assays

Bafilomycin A1 (200 nmol/L) was used to inhibit autophagic degradation. MG132 (10 μmol/L) was used to inhibit proteasome-mediated protein degradation.

2.12. Flow cytometry analysis

For cultured cell membrane PD-L1 analysis, cells subjected to the indicated treatments were collected and incubated with APC-conjugated anti-mouse PD-L1 antibody (BioLegend, Clone: 10F.9G2, 124312) on ice for 20 min. For tumor-infiltrating T-cell profile analysis, excised tumors were digested in digestion buffer (200 U/mL collagenase IV and 100 μg/mL DNA I in HBSS buffer). Lymphocytes were enriched on a Ficoll gradient. After blocking with an anti-CD16/CD32 (BioLegend; Clone: 93, 101301) antibody, the cells were stained with APC-conjugated anti-mouse CD45 (BioLegend, Clone: 30-F11, 103111), PerCP/Cyanine5.5-conjugated anti-mouse CD3 (BioLegend, Clone: 145-2C11, 100328), and APC-Cy7-conjugated anti-mouse CD8 (BioLegend, Clone: 53-6.7, 100714) antibodies for 20 min. After fixation and permeabilization with fixation/permeabilization buffer, intracellular IFNγ was stained with PE-Cy7-conjugated anti-mouse IFNγ (BioLegend, Clone: XMG1.2, 505826) antibody, and Granzyme B was stained with PE-Cyanine 7-conjugated anti-mouse/human Granzyme B (BioLegend, Clone: QA16A02, 372213) antibody. The stained cells were analyzed by a BD FACSVerse™ flow cytometer (BD Biosciences, USA). For other tumor-infiltrating innate immune cell analyses, the following mAbs were used: FITC-conjugated anti-mouse CD45 (BioLegend, Clone: 30-F11, 103108), PerCP/Cyanine5.5-conjugated anti-mouse/human CD11b (BioLegend, Clone: M1/70, 101228), PE-conjugated anti-mouse Gr-1 (BioLegend, Clone: RB6-8C5, 108407), PE-conjugated anti-mouse F4/80 (BioLegend, Clone: BM8, 123110), Brilliant Violet 605™-conjugated anti-mouse Ly-6G (BioLegend, Clone: 1A8, 127639), Brilliant Violet 421™-conjugated anti-mouse CD11c (BioLegend, Clone: N418, 117343), and PE-conjugated anti-mouse CD49b (BioLegend, Clone: DX5, 108907). The stained cells were analyzed by a BD FACSCelesta™ or a BD FACSVerse™ flow cytometer (BD Biosciences, USA). The data were further analyzed by FCS Express 6.

2.13. Cell proliferation

According to the manufacturer's instructions, cell proliferation was measured using a CCK-8 kit (Dojindo Inc., Kumamoto, Japan). Briefly, cells were plated in 96-well plates and treated with the indicated PKCα inhibitors. At the indicated time points (24, 48, and 72 h), a mixture of 10 μL of the CCK-8 solution and 90 μL of culture medium was added to each well, after which the absorbance was measured at 450 nm using a microplate reader.

2.14. PD-L1 and PD-1 binding assay

To measure the interaction between PD-1 and PD-L1, cells were fixed in 4% paraformaldehyde at room temperature for 20 min and then incubated with human PD-1 Fc protein (R&D Systems) for 2 h, followed by incubation with anti-human Alexa Fluor 488 secondary antibodies (Life Technologies) at room temperature for 1 h. After being incubated with DAPI, the cells were visualized with a confocal fluorescence microscope (Olympus, CA, USA).

2.15. T-cell mediated tumor cell killing assay

C57BL/6-Tg(TcraTcrb)1100Mjb/J mice (OT-I mice) were purchased from Shanghai Biomodel Organism Science & Technology Development Co., Ltd. The SIINFEKL peptide (OVA257-264) was purchased from Sigma−Aldrich. The spleen was homogenized, and single cells were suspended in 1 × red blood cell lysis buffer (Sigma−Aldrich) for 2 min. The splenocytes were centrifuged and washed, and the $CD8^+$ T cells were purified using an EasySep Mouse $CD8^+$ T-Cell Isolation Kit (Stemcell). The T cells were then resuspended in RPMI culture medium supplemented with 5 μg/mL OVA257-264 peptide, 10 ng/mL mouse recombinant IL-2, and 50 μmol/L β-mercaptoethanol. After five days of activation, the OT-I $CD8^+$ T cells were collected, OVA-expressing 4T1 cells (4T1 OVA) were allowed to adhere to the plates overnight, and OT-I cells were then added to the culture at a ratio of 5:1. To determine the percentage of dead cells, all cells were collected by trypsinization, stained with 7-AAD, and analyzed by a BD FACSCelesta flow cytometer.

2.16. MDA-MB-231 xenograft mouse model

Six-week-old female NOD-SCID mice were purchased from HFK Bioscience Co., Ltd. (Beijing, China). A total of 1.5×10^6 MDA-MB-231 cells transfected with either Ctrl-shRNA or *PKCα*-shRNAs were subcutaneously (s.c.) injected into the mammary fat pads of NOD-SCID mice. Tumors were measured every seven days with a caliper, and tumor volume was calculated using Eq. (1):

$$\text{Tumor volume} = 1/2 \times \text{Length} \times \text{Width}^2 \quad (1)$$

2.17. 4T1 allograft mouse model

Six-week-old female BALB/c mice (HFK Bioscience, Beijing, China) and NCG mice (GemPharmatech, Nanjing, China) were maintained in the animal facility at the Institute of Materia Medica under specific-pathogen-free conditions. A total of 3 or 5×10^5 4T1 cells transfected with either Ctrl-shRNA or *Pkcα*-shRNA were injected into the mammary fat fads. Tumors were measured every seven days with a caliper, and tumor volume was calculated using Eq. (1). For treatment with antibodies, 100 μg of anti-PD-L1 antibody or control rat IgG was injected intraperitoneally twice a week beginning on Day 7 for 3 times. For PKC inhibitor treatment, the PKCα inhibitor Go6976 (2 mg/kg/day), the PKCβ inhibitor enzastaurin (5 mg/kg/day), or the PKC-θ inhibitor compound **20** (5 mg/kg/day) was injected intraperitoneally beginning on Day 7 after tumor cell inoculation. For CD8 depletion, 100 μg of anti-mouse CD8 antibody or rat IgG2b isotype control was intraperitoneally injected twice a week beginning on Day 4 after tumor inoculation. To block activated lymphocyte trafficking to tumor tissues, mice were intravenously injected with 25 μg of FTY720 on Day 0 after tumor inoculation. Then, 5 μg of FTY720 was given every day to maintain inhibition.

2.18. Bioinformatics analysis

The mRNA expression data of *PRKCA* in different subtypes of breast cancer cells or tissues were extracted from published gene expression data available in the GEO database (GSE12790). Comparisons of *PRKCA* expression between tumor and normal tissues, as well as among pathological stages, were performed on the following website: http://gepia.cancer-pku.cn. Correlations between *CD274* and *PRKCA* mRNA expression across TCGA lung cancer datasets were also analyzed with the GEPIA database. The KM plotter breast cancer dataset was obtained from http://kmplot.com/analysis. PKCα-mediated PD-L1 phosphoprotein sites were predicted by NetPhos 3.1 (https://services.healthtech.dtu.dk/services/NetPhos-3.1/) and GPS5.0 (http://gps.biocuckoo.cn). The sequence alignment of PD-L1 from different species was achieved with the online PRALINE toolkit (https://www.ibi.vu.nl/programs/pralinewww/). The correlation between *PRKCA* expression and $CD8^+$ T-cell infiltration (http://timer.cistrome.org) in different subtypes of breast cancer patients was analyzed using the Timer database. The mRNA expression of *PRKCA*, *PRKCB*, and *PRKCQ* in a diverse panel of human breast cancer cell lines was analyzed by using the Human Protein Atlas database (https://www.proteinatlas.org). The amplification frequency of PKCα in the TCGA invasive breast carcinoma dataset (TCGA, Firehose Legacy) was analyzed by using cBioPortal (https://www.cbioportal.org).

2.19. Study approval

All animal studies were approved by the Animal Experimentation Ethics Committee of the Chinese Academy of Medical Sciences. All procedures were conducted following the Institutional Animal Care and Use Committees of the Chinese Academy of Medical Sciences guidelines. The animal study also complied with the ARRIVE guidelines[40]. A human breast cancer microarray (HBreD050Bc01) was purchased from Shanghai Outdo Biotech Company, with the authority granting the ethics approval number SHYJS-CP-1910003.

2.20. Statistical analysis

The data are presented as the mean ± standard error of mean (SEM). The statistical significance of differences between two groups was determined by an unpaired two-tailed Student's *t*-test. Statistical significance among three or more groups was determined by one-way ANOVA. The correlation between groups was determined by Pearson's correlation test. The survival rates were analyzed using Kaplan−Meier analysis. Generally, all the experiments were carried out with $n \geq 3$ biological replicates. All the statistical analyses were performed using GraphPad Prism 8.0 software. $P < 0.05$ was considered to indicate statistical significance.

3. Results

3.1. Inhibition of PKCα abolishes antitumor activity in immunocompetent mice

PKCα has long been considered an oncogene and potential therapeutic target for cancer therapy[8,9]. Although many PKCα inhibitors or specific antisense oligonucleotides have been developed and tested in clinical trials, none of them have been approved yet due to unsatisfactory clinical efficacy[11]. Systems biology and the concept of "Biao Ben Jian Zhi" helped to reconsider these issues during drug discovery by integrating expertise from diverse fields and perspectives[41-43]. The high efficacy of *in vitro* studies and some *in vivo* preclinical models and the frustration of PKCα-targeting oncology clinical trials prompted us to address these inconsistency issues, especially by refining or rethinking the most

common therapeutic models currently used in preclinical studies of breast cancer. Considering that greater transcription of *PRKCA*, the gene encoding PKCα, was detected in basal-like breast cancer tissues and cell lines than in luminal and *HER2* amplified counterparts (Fig. 1A and B, Supporting Information Fig. S1A), we focused mainly on the functional role of PKCα in aggressive triple-negative breast cancer. We first used a specific small hairpin RNA (shRNA) to silence *PKCα* in two types of breast cancer cell

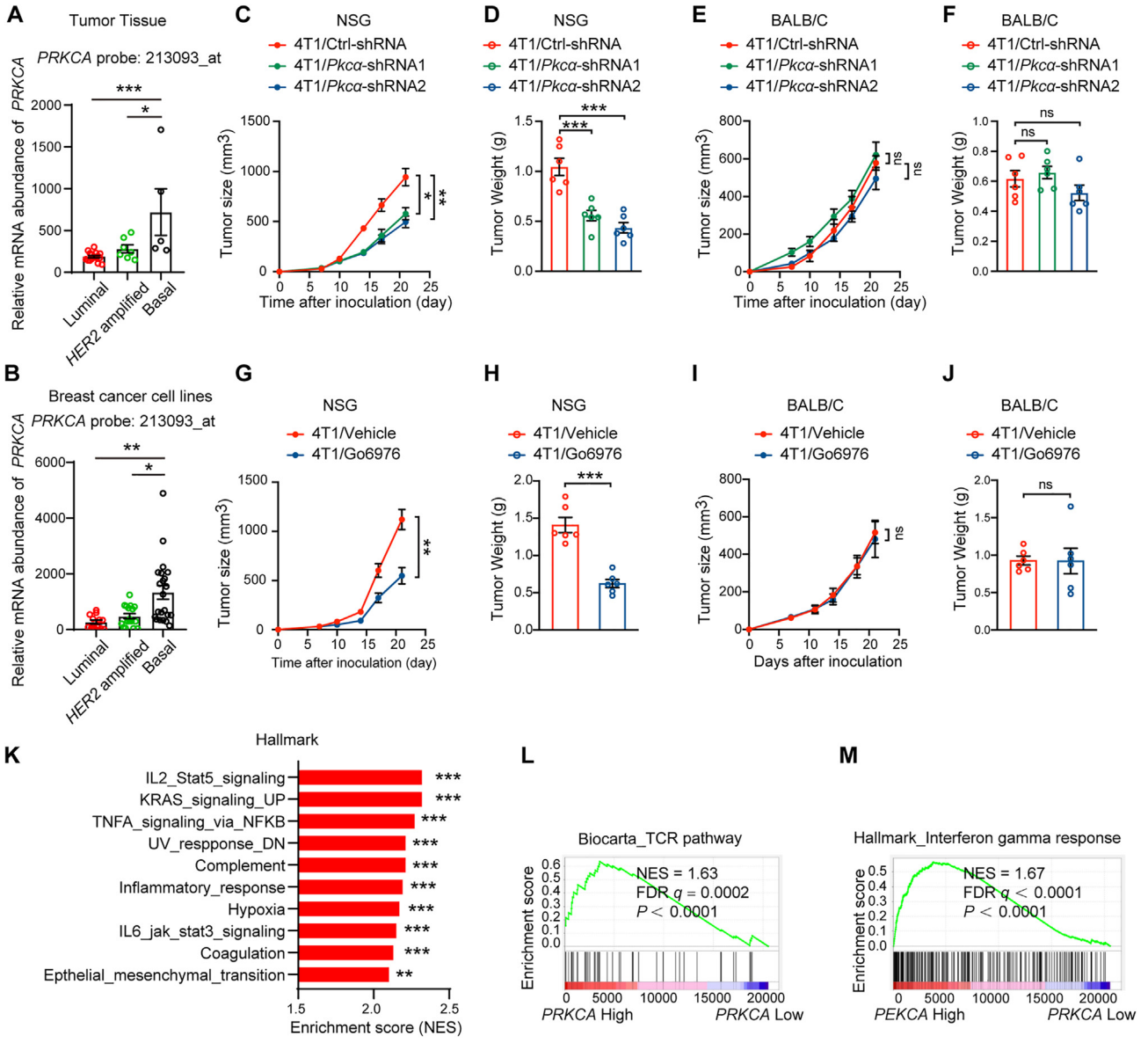

Figure 1 PKCα inhibition abolishes antitumor activity in immunocompetent mice. (A) Expression data for *PRKCA* were extracted from published gene expression data on breast cancer tissues available in the GEO database (GSE12790) ($n = 5-17$). Relative *PRKCA* transcript levels were measured using the 213093_at probe. (B) Expression data for *PRKCA* were extracted from published gene expression data on breast cancer cell lines available in the GEO database (GSE12790). Relative *PRKCA* transcript levels were measured using the 213093_at. (C–F) NCG mice (C, D) or BALB/c mice (E, F) were subcutaneously (s.c.) inoculated into mammary fat pads, and 4T1 cells were stably transfected with the indicated shRNA directed against *Prkca* or with a scrambled sequence as a control. The graphs depict the tumor volumes (C, E) or tumor weights (D, F) of mice given s.c. injections of 5×10^5 of the indicated cells ($n = 6$). (G–J) NCG mice (G, H) or BALB/c mice (I, J) were subcutaneously (s.c.) injected into mammary fat pads with 5×10^5 4T1 cells and then treated with the PKCα inhibitor Go6976 or vehicle. The graphs depict the tumor volumes (G, I) or tumor weights (H, J) ($n = 6$). (K) GSEA demonstrating the enrichment of gene sets related to hallmark genes in the ranked gene list of the *PRKCA*-High group (the top 10th percentile, $n = 122$) *versus* the *PRKCA*-Low group (the bottom 10th percentile, $n = 122$) of breast cancer patients expressing *PRKCA* from the TCGA database ($n = 1218$). The top ten pathways, together with their enrichment scores, are depicted. NES, normalized enrichment score. (L, M) GSEA demonstrating the enrichment of gene sets related to the TCR pathway (L) and interferon-gamma response (M) in the ranked gene list of the top 10th percentile ($n = 122$) *versus* the bottom 10th percentile ($n = 122$) of breast cancer patients expressing *PRKCA* from the TCGA database ($n = 1218$). NES, normalized enrichment score. FDR, false discovery rate. The results are presented as the mean ± SEM. $^*P < 0.05$, $^{**}P < 0.01$, $^{***}P < 0.001$, ns means not significant.

lines, human MDA-MB-231 cells and mouse 4T1 cells (Fig. S1B). As expected, silencing *PKCα* in MDA-MB-231 cells or *Pkcα* in 4T1 cells significantly reduced tumor proliferation *in vitro* (Fig. S1C). We then ranked 20530 genes from 1218 breast cancer samples in the TCGA dataset by relative *PRKCA* expression in the top 10th percentile (*PRKCA*_high) versus the bottom 10th percentile (*PRKCA*_low) for gene set enrichment analysis (GSEA). Pro-survival gene sets such as MAPK/ERK pathway and PI3K/AKT pathway were enriched in the *PRKCA*_high tumor samples (Fig. S1D and S1E). Moreover, the PKCα kinase inhibitors Go6976 and Ro-32-0432 suppressed pro-survival AKT and ERK signaling and inhibited the proliferation of MDA-MB-231 cells and 4T1 cells *in vitro* (Fig. S1F−S1H), supporting the oncogenic role of PKCα in promoting breast cancer proliferation *in vitro*. The protumor role of PKCα was validated in an *in vivo* MDA-MB-231 xenograft model (Fig. S1I). Consistent with the findings of previous studies[44-46], the increase in tumor growth induced by *PKCα* overexpression can be abolished by the AKT inhibitor MK2206 or the ERK inhibitor U0126 (Fig. S1J), indicating that PKCα promotes breast cancer cell proliferation *in vitro* through the AKT and ERK signaling axes.

Considering the influences of the immune system, we also conducted allograft experiments and compared the efficacy between immunocompetent mice and immunodeficient mice as previously described[47,48]. We subcutaneously inoculated 5×10^5 *Pkcα*-shRNA- or Ctrl-shRNA-transfected 4T1 cells into the mammary fat pads of immunodeficient NCG mice and immunecompetent BALB/c mice. Silencing *Pkcα* expression suppressed tumor growth in immunodeficient mice (Fig. 1C and D) but not in immunocompetent mice (Fig. 1E and F). Consistently, the PKCα inhibitor Go6976 suppressed tumor growth in NCG mice (Fig. 1G and H) but not in BALB/c mice (Fig. 1I and J). These results indicate that an intact immune system may compromise the antitumor efficacy of PKCα inhibition.

We then analyzed clinical outcomes based on the transcription of *PRKCA* in patients with breast cancer *via* the GEPIA and Kaplan−Meier plotter databases. We queried the TCGA breast cancer dataset from the GEPIA database for information on 1085 patients with breast cancer. These patients expressed lower levels of PRKCA than did their normal counterparts ($n = 291$) (Supporting Information Fig. S2A). However, the expression of *PRKCA* did not significantly differ among breast cancer patients at different stages (Fig. S2B). Patients with tumors exhibiting lower PKCα mRNA (*PKCα*-low) or PKCα protein (PKCα-low) expression had significantly shorter relapse-free survival or overall survival than patients with tumors exhibiting high PKCα mRNA or PKCα protein expression (Fig. S2C and S2D). There was a significantly lower proportion of patients with favorable prognostic features in the *PKCα*-low subgroup than in the PKCα-high subgroup for the luminal A and basal subtypes (Fig. S2E). These surprising clinical analysis results indicated the dual oncological roles of PKCα, additional evidence that simply targeting PKCα may not work in clinical studies.

We further performed GSEA of breast cancer patients in the TCGA dataset with hallmark gene sets. The *PRKCA*_high tumor samples were enriched in the expression of gene signatures associated with several inflammation-related gene sets, such as those related to the inflammatory response, TNFα signaling *via* NFκB and IL-2_STAT5 signaling, in comparison with the *PRKCA*_low samples (Fig. 1K). GSEA also revealed significant enrichment of immune effector gene pathways, including the TCR pathway, interferon-gamma (IFNγ) response, adaptive immune response, T-cell activation, cytokine production, and cytokine pathway in tumor tissues with high *PKCα* expression (Fig. 1L and M, Supporting Information Fig. S3A). Therefore, we propose that the failure of PKCα inhibitors in cancer treatment may be related to a reduction in the antitumor immune response in PKCα-targeted patients.

To verify this hypothesis, we first evaluated the effect of PKCα on the infiltration of innate immune cells. We detected the proportions of innate immune cells, including myeloid-derived suppressor cells, macrophages, neutrophils, dendritic cells, and natural killer cells, in *Pkcα*-shRNA- or Ctrl-shRNA-transfected 4T1 tumors. The proportions of these innate immune cells in tumor tissues were comparable among the different groups, which excluded the contribution of these innate immune cells (Fig. S3B and S3C). $CD8^+$ T cells play critical roles in antitumor immunity by releasing cytotoxic molecules such as granzyme B and perforin and producing IFNγ to enhance the expression of MHC class I. We then monitored the activation of $CD8^+$ T cells by assessing the proportions of $IFN\gamma^+$ $CD8^+$ T cells and granzyme B^+ $CD8^+$ T cells among all $CD8^+$ cells. Silencing *Pkcα* indeed decreased the proportion of activated $CD8^+$ T cells (Fig. 2A and B, Supporting Information Fig. S4A). Moreover, the PKCα inhibitor Go6976 significantly reduced the percentage of $IFN\gamma^+$ $CD8^+$ T and granzyme B^+ $CD8^+$ T cells (Fig. 2C).

To validate whether the antitumor effect of PKCα inhibition is dependent on $CD8^+$ T cells, we used a neutralizing anti-CD8α monoclonal antibody (mAb) to deplete $CD8^+$ T cells (Fig. 2D). In mice inoculated with Ctrl-shRNA-transfected 4T1 cells, compared with immunoglobulin G2b (IgG2b) isotype control treatment, anti-CD8α mAb treatment decreased TILs, suppressed $CD8^+$ T-cell infiltration (Fig. S4B) and enhanced tumor growth (Fig. 2D−F), which is consistent with the findings of previous studies[49]. Notably, in the CD8 depletion study, silencing *Pkcα* in 4T1 cells slowed tumor progression, as indicated by a decrease in tumor volume (Fig. 2D−F). Furthermore, we utilized FTY720 to block activated lymphocyte trafficking to tumor tissues. Similarly, silencing *Pkcα* significantly decreased the tumor burden in mice that received FTY720 (Fig. S4C−S4F). Collectively, these results indicate that the effect of PKCα inhibition (tumor-suppressing versus tumor-promoting) depends on the presence of $CD8^+$ T cells.

3.2. *PKCα interacts with PD-L1 and suppresses PD-L1 expression*

Immune checkpoint gene expression on tumor cells plays a vital role in tumor evasion. To investigate whether the inhibition of PKCα-induced immune invasion is mediated by immune checkpoints, we first detected the expression levels of immune checkpoint molecules in human MDA-MB-231 and mouse 4T1 cells. *PKCα* depletion dramatically increased the expression of PD-L1 but not the other immune inhibitory ligands (Fig. 3A and Supporting Information Fig. S5A). Indeed, we identified PKCα as a binding partner of PD-L1 by immunoprecipitation coupled with mass spectrometry (Fig. S5B−S5D). The interaction between PKCα and PD-L1 was further confirmed by coimmunoprecipitation (Fig. 3B) and confocal microscopy (Fig. 3C). Compared to those in MDA-MB-231 and BT549 cells, the mRNA expression and protein abundance of PKCα in MDA-MB-468 cells were significantly lower (Fig. 3D and Fig. S5E). Overexpression of PKCα in MDA-MB-468 cells decreased the expression of PD-L1, and silencing of PKCα in BT549 cells increased the expression of

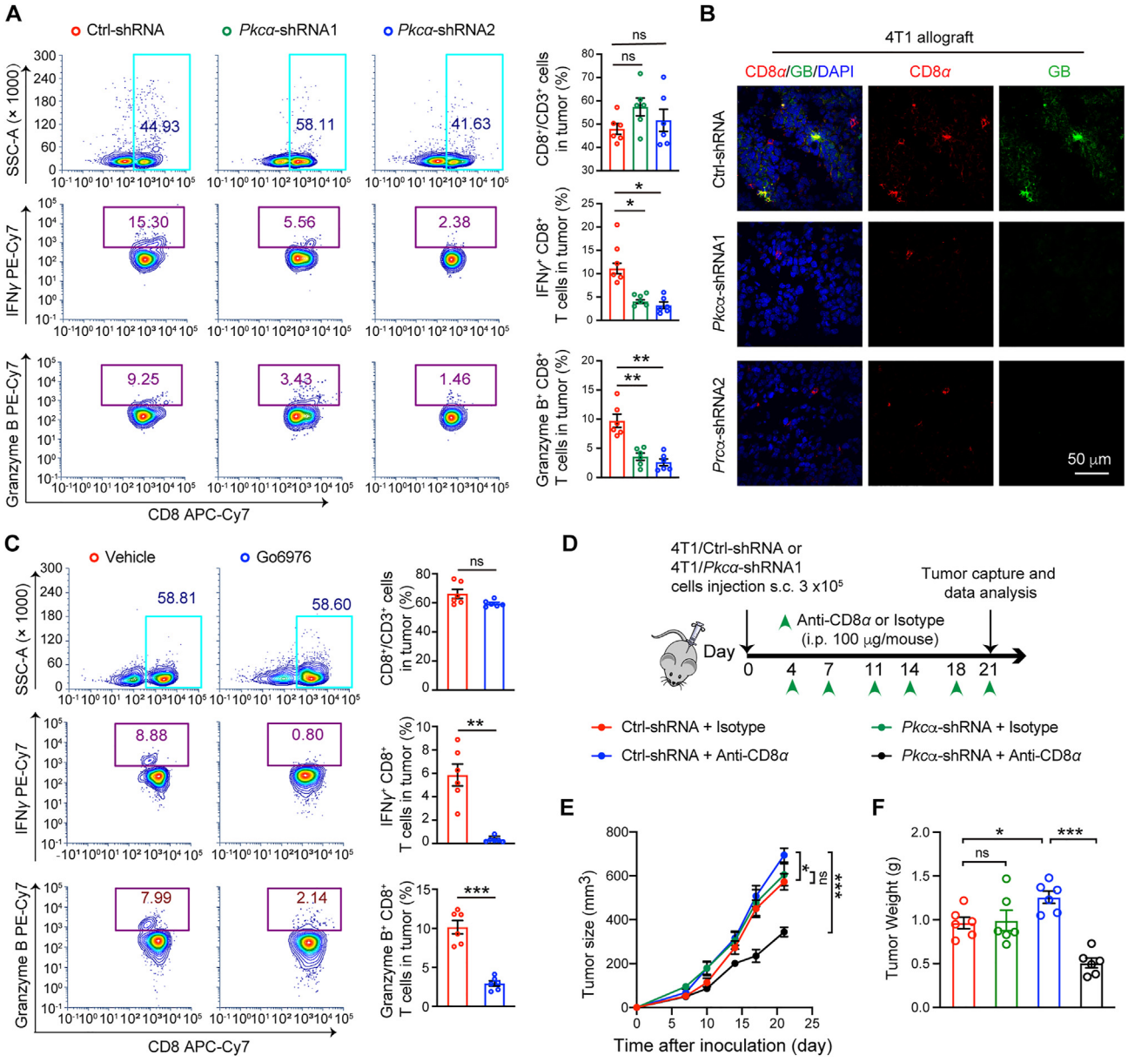

Figure 2 Inhibition of PKCα enhances $CD8^+$ T-cell-mediated tumor evasion. (A) Flow cytometric assays (left) and quantification (right) showing the percentages of $CD8^+$ cells among $CD3^+$ T cells (top), $IFN\gamma^+$ cells among $CD8^+$ T cells (middle), and granzyme B^+ cells among $CD8^+$ T cells (bottom) from allograft tumors derived from animals implanted with 4T1 cells transfected with either Ctrl-shRNA or *Pkcα*-shRNAs. (B) Expression of Cd8α or granzyme B was detected by immunofluorescence staining in allograft tumors from mice implanted with 4T1 cells transfected with either Ctrl-shRNA or *Pkcα*-shRNAs. (C) Flow cytometric assays (left) and quantification (right) of the percentages of $CD8^+$ cells among $CD3^+$ T cells (top), $IFN\gamma^+$ $CD8^+$ cells (middle), and granzyme B^+CD8^+ cells (bottom) among $CD8^+$ T cells from 4T1 allograft tumors treated with either the PKCα inhibitor Go6976 or vehicle. (D–F) BALB/c mice implanted with 4T1 cells transfected with either Ctrl-shRNA or *Pkcα*-shRNA1 were treated with an anti-CD8α mAb or an IgG2b isotype control. (D) A schematic view of the treatment plan. (E) Tumor volumes over time (days). (F) Weights of the tumors excised from each group. The results are presented as the mean ± SEM. $^*P < 0.05$, $^{**}P < 0.01$, $^{***}P < 0.001$, ns means not significant.

PD-L1 (Fig. 3E). Moreover, the expression of PD-L1 was elevated in allograft tumors from mice implanted with 4T1 cells transfected with *Pkcα*-shRNAs (Fig. 3F). Similarly, treatment with PKCα inhibitors such as Go6976, Go6850 or Ro-32-0432 enhanced PD-L1 expression in a dose-dependent manner in MDA-MB-231 (Fig. 3G) and 4T1 (Fig. S5F) cells. A negative correlation was observed between PKCα and PD-L1 protein levels in primary breast tumor tissues (Fig. S5G). Moreover, PKCα inhibition with Go6976 or Ro-32-0432 stabilized PD-L1 in the cell plasma, as detected by flow cytometry (Fig. S5H). We then investigated whether the downregulation of PKCα in tumor cells enhances PD-1 binding. As expected, the binding of PD-1 to MDA-MB-231 cells transfected with *PKCα*-shRNAs was enhanced (Fig. 3H). Consistent with these findings, T-cell-mediated cytotoxicity toward tumor cells was suppressed in 4T1 cells transfected with *Pkcα*-shRNAs, and depletion of *Pd-l1* in *Pkcα*-knockdown tumor cells reversed

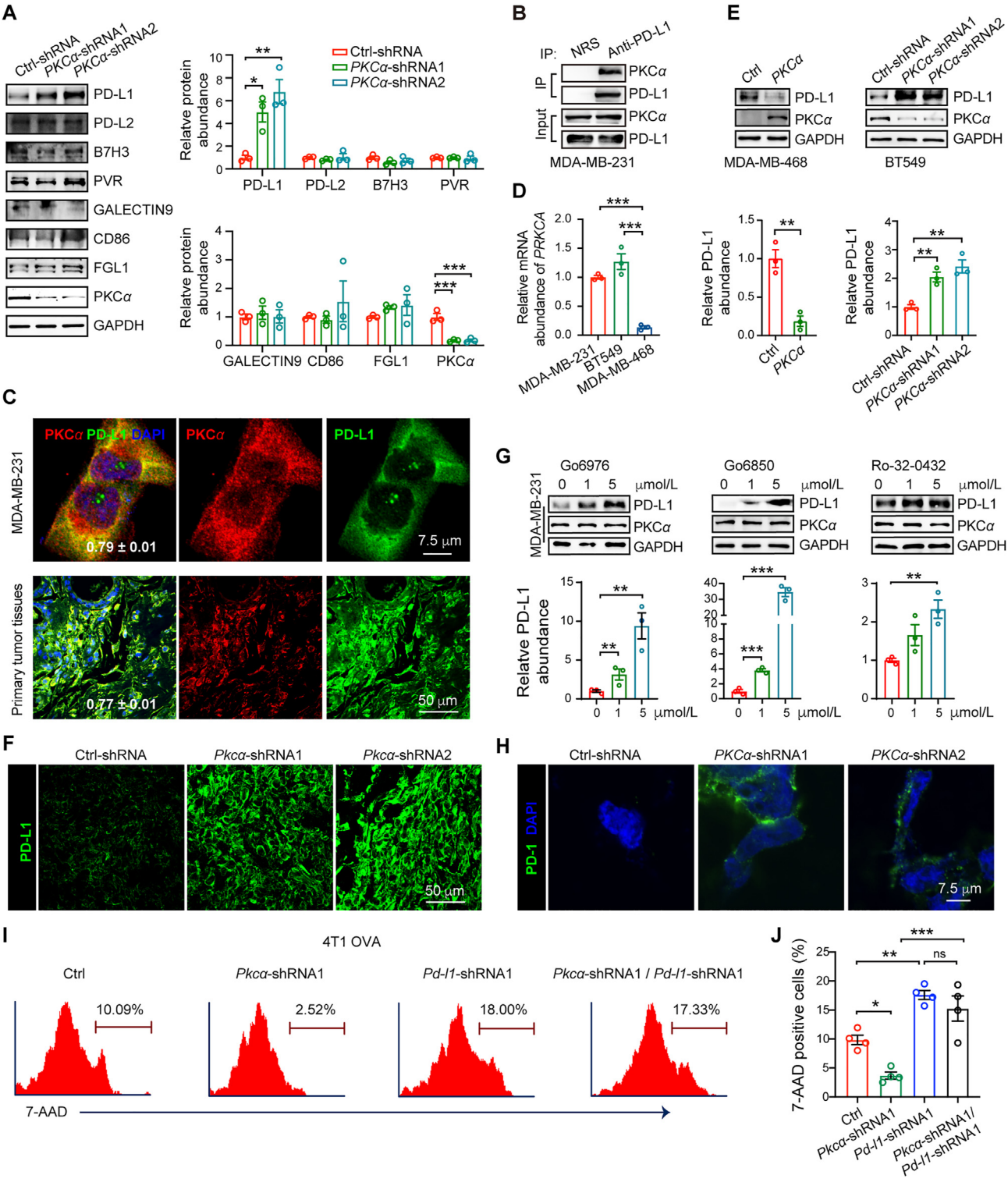

Figure 3 PKCα interacts with PD-L1 and suppresses PD-L1 expression. (A) Immunoblotting (IB) and quantitative analyses of the expression of immune checkpoints in MDA-MB-231 cells transfected with Ctrl-shRNA or *PKCα*-shRNAs, as indicated at the top. (B) Coimmunoprecipitation (co-IP) of MDA-MB-231 cell lysates using normal rabbit serum (NRS) or an anti-PD-L1 antibody (Ab) was performed for immunoblotting analyses probed with an antibody specific for PKCα or PD-L1. (C) The colocalization of PKCα with PD-L1 was detected by immunofluorescence staining of MDA-MB-231 cells ($n = 6$) and primary breast tumor tissues ($n = 20$). The quantification of PKCα/PD-L1 colocalization is shown as the Pearson's coefficient. (D) Quantitative real-time PCR analysis of *PRKCA* in MDA-MB-231, BT549, and MDA-MB-468 cells. (E) IB and quantitative analyses of protein lysates from MDA-MB-468 or BT549 cells (as indicated at the bottom) transfected with the indicated overexpression plasmids or shRNAs (as indicated at the top). (F) The expression of PD-L1 in allograft tumors from mice implanted with 4T1 cells transfected with either Ctrl-shRNA or *Pkcα*-shRNAs was detected by immunofluorescence staining. (G) IB and quantitative analyses of the

this effect (Fig. 3I and J). Taken together, these results indicate that targeting PKCα enhances tumor evasion by enhancing PD-L1 expression and reducing T-cell activity.

3.3. PKCα-mediated PD-L1 phosphorylation promotes PD-L1 degradation through β-TRCP

We next investigated how PKCα inhibition upregulates PD-L1 expression in breast cancer. We first queried the TCGA database and found no apparent correlation between the expression of *PRKCA* and *CD274* (encoding PD-L1) at the transcriptional level in breast cancer tissues (Fig. 4A). Moreover, silencing *PKCα* did not affect *CD274* at the transcript level in MDA-MB-231 cells (Fig. 4B). These results indicated that PKCα has no effect on *CD274* transcription. Next, we used cycloheximide to suppress protein synthesis. Silencing *PKCα* or pharmacological inhibition of PKCα by Go6976 increased the half-life of PD-L1 from 6.6 or 5.8 h, respectively, to more than 24 h in MDA-MB-231 cells (Fig. 4C and Supporting Information Fig. S6A), whereas overexpression of PKCα reduced the half-life of PD-L1 from 9.9 to 2.9 h in MDA-MB-468 cells (Fig. S6B), suggesting that PKCα is involved in downregulating PD-L1 stabilization.

Since PD-L1 is a binding partner of PKCα, we then asked whether PD-L1 is a kinase substrate of PKCα. Coimmunoprecipitation assays indicated that ectopically expressed PKCα induced apparent phosphorylation of PD-L1 (Fig. S6C), which mainly occurred at serine residues (Fig. 4D). PKCα-mediated PD-L1 phosphorylation promoted PD-L1 ubiquitination and degradation through the ubiquitin−proteasome system (Fig. 4E and Fig. S6D). The NetPhos 3.1 and GPS 5.0 databases were used to predict the potential phosphorylation sites in PD-L1 by PKCα, and the candidate serine phosphorylation sites were PD-L1^{S80}, PD-L1^{S184} and PD-L1^{S279} (Fig. 4F). To verify the critical serine site on PD-L1, we subsequently mapped the region in which PD-L1 interacts with PKCα (Fig. 4G). GFP-tagged PD-L1 deletion mutants were constructed and subjected to coimmunoprecipitation. The results showed that PKCα selectively bound to the extracellular domain of PD-L1 (Fig. 4G). We selected S80 and S184 in the extracellular domain of PD-L1 for subsequent analysis. Notably, S184 is highly conserved across different species (Fig. S6E). Mutation of PD-L1 S184 to a phosphorylation-resistant alanine residue abrogated PD-L1 degradation, but the S80A mutation did not affect PD-L1 stability (Fig. S6F). Moreover, the S184A variant of PD-L1 lost its ability to be phosphorylated by PKCα, suggesting that PKCα may decrease PD-L1 expression by phosphorylating PD-L1^{S184} (Fig. 4H). Consistent with this notion, compared with the reduction in the expression of wild-type PD-L1, the overexpression of PKCα had no impact on the expression of the PD-L1 S184A mutant in MDA-MB-468/*CD274* KO cells (Fig. S6G).

Glycogen synthase kinase 3β reportedly phosphorylates PD-L1 at T180 and S184, leading to polyubiquitination and proteasome degradation of PD-L1 by β-TRCP[33]. We hypothesized that PKCα-mediated PD-L1^{S184} phosphorylation might also promote PD-L1 degradation in a β-TRCP-dependent manner. We first knocked down *β-TRCP* in MDA-MB-231 cells. Silencing *β-TRCP* increased PD-L1 expression but had no effect on PKCα expression, suggesting that β-TRCP mediates PD-L1 degradation without affecting PKCα expression (Fig. S6H). Moreover, the expression of β-TRCP was comparable between control cells and PKCα-silenced cells, indicating that PKCα does not regulate β-TRCP expression (Fig. S6I). We also investigated whether PKCα promoted the interaction of β-TRCP with PD-L1. Overexpression of *PKCα* enhanced the β-TRCP/PD-L1 interaction and thereby accelerated β-TRCP-mediated PD-L1 ubiquitination (Fig. 4I and Fig. S6J). Furthermore, the expression of PD-L1 could not be reduced by ectopic expression of PKCα under *β-TRCP*-silencing conditions (Fig. 4J). These results indicated that PKCα-mediated PD-L1 phosphorylation promotes PD-L1 degradation in a β-TRCP-dependent manner.

3.4. Synergistic effects of PKCα inhibition and anti-PD-L1 mAb therapy in a preclinical breast cancer mouse model

We further assessed whether anti-PD-L1 mAb therapy enhanced the therapeutic effect of PKCα knockdown. Consistent with our observations above, the volume of allograft tumors in the *Pkcα*-shRNA1 group was not significantly different from that in the Ctrl-shRNA group (Fig. 5A−C). Similarly, the 4T1-engrafted mice were poorly responsive to the Go6976 treatment (Fig. 5D−F). Consistent with previous findings[50], anti-PD-L1 mAb treatment significantly decreased the tumor volume compared to that in the isotype control group (Fig. 5A−F). More importantly, anti-PD-L1 mAb treatment enhanced the sensitivity to *PKCα* gene knockdown (Fig. 5A−C) or the PKCα inhibitor Go6976 (Fig. 5D−F), suggesting that anti-PD-L1 mAb treatment robustly synergized with PKCα-targeting therapy (Fig. 5A−F). Moreover, we observed that PKCα inhibition enhanced PD-L1 expression (Fig. 5G and H) and reduced the percentage of tumor-infiltrating cytotoxic CD8$^+$ T cells (Fig. 5I). In addition, the expression of proteins involved in PKCα-mediated proliferation signaling pathways, such as ERK and AKT, was downregulated in *Pkcα*-shRNA1 tumors and *Pkcα*-shRNA1 tumors treated with PD-L1 (Supporting Information Fig. S7). This ERK and AKT signaling inhibition was also observed in both the Go6976-treated group and the combination-treated group (Fig. 5J). Taken together, these results indicate that PD-L1 blockade restores the antitumor effects of PKCα-targeted therapy.

To further assess whether CD8$^+$ T cells contribute to the synergistic effect of the combination therapy, we used an anti-CD8α mAb to block CD8$^+$ T cells for *in vivo* experiments. The anti-CD8α mAb enhanced the tumor burden in mice that received combination treatment with Go6974 and the anti-PD-L1 mAb (Fig. 6A−C). In addition, CD8$^+$ T-cell infiltration was reduced in mice treated with the anti-CD8α mAb (Fig. 6D and E). Hence, CD8$^+$ T cells are essential immune effectors for *PKCα* deficiency-mediated antitumor immunity, and the efficacy of PKCα inhibitors was intensified by synergizing with anti-PD-L1 mAb therapy to boost antitumor T-cell immunity *in vivo*.

expression of PD-L1 and PKCα in MDA-MB-231 cells that received three different PKCα inhibitor treatments, as indicated at the top. (H) PD-1 binding assay in MDA-MB-231 cells transfected with Ctrl-shRNA or *PKCα*-shRNAs, as indicated at the top. (I, J) Representative plots (I) and statistical analyses (J) of the results of the T-cell-mediated tumor cell killing assay in 4T1 OVA cells transfected with the indicated plasmids. The results are shown as the percentages of 7-AAD$^+$ tumor cells. The results are presented as the mean ± SEM. *$P < 0.05$, **$P < 0.01$, ***$P < 0.001$, ns means not significant.

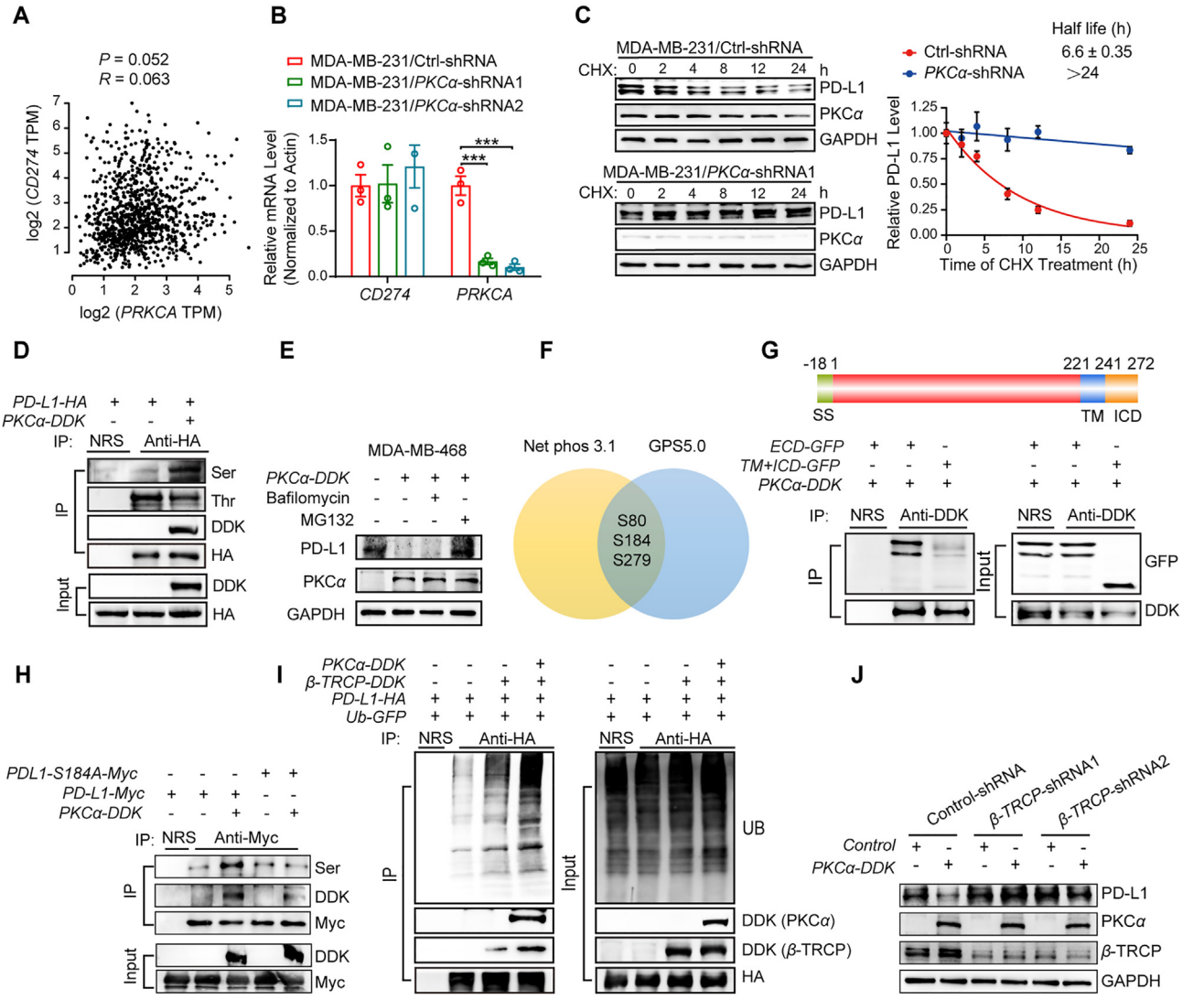

Figure 4 PKCα-mediated PD-L1 phosphorylation promotes PD-L1 degradation through β-TRCP. (A) Pearson's correlation analysis between *PRKCA* and *CD274* mRNA expression across TCGA breast carcinoma (BRCA) datasets retrieved from the GEPIA website. (B) *PD-L1* (*CD274*) and *PKCα* (*PRKCA*) mRNA expression in MDA-MB-231 cells transfected with Ctrl-shRNA or *PKCα*-shRNAs. (C) Effect of PKCα depletion on PD-L1 degradation *in vitro*. MDA-MB-231 cells transfected with Ctrl-shRNA or *PKCα*-shRNAs were incubated with 20 μmol/L cycloheximide (CHX) for the indicated times. (D) Co-IP of HEK293 cell lysates using NRS or an anti-HA Ab was performed for IB analyses probed with antibodies specific for phosphoserine, phosphothreonine, DDK, or HA. (E) Control or *PKCα-DDK*-expressing MDA-MB-468 cells were incubated with 200 nmol/L bafilomycin or 10 μmol/L MG132 for 8 h. The indicated proteins were analyzed using IB analysis. (F) Venn diagram indicating the overlap of PKCα-mediated PD-L1 phosphoprotein sites predicted by NetPhos 3.1 and GPS5.0. (G) Mapping the PD-L1 regions that bind to PKCα (upper). *PKCα-DDK*-expressing HEK293T cells were cotransfected with the indicated PD-L1-ECD-GFP or PD-L1-TM-ICD-GFP constructs. Cell extracts were immunoprecipitated with NRS or an anti-DDK Ab and then probed with an anti-GFP Ab or an anti-DDK Ab (bottom). (H) Lysates from HEK293T cells transfected with the indicated plasmids were immunoprecipitated with NRS or an anti-Myc Ab. IB shows the phosphorylation of PD-L1 and the PD-L1 S184A mutant. (I) Effect of β-TRCP and PKCα on PD-L1 ubiquitination. HEK293 cells transfected with the indicated plasmids were immunoprecipitated with NRS or an anti-HA Ab. The ubiquitination of PD-L1 was detected by IB. (J) IB showing the expression of PD-L1, PKCα, and β-TRCP in MDA-MB-468 cells transfected with Ctrl-shRNA or *β-TRCP*-shRNAs, as indicated at the top. The results are presented as the mean ± SEM. ***$P < 0.001$.

3.5. PKCα expression is correlated with immune gene signatures in cancer patients

To further validate our observations in patients with breast cancer, we investigated whether PKCα is correlated with $CD8^+$ cytotoxic T-cell infiltration in primary human breast cancer. Immunofluorescence staining revealed that PKCα expression was positively associated with $CD8^+$ T-cell infiltration and granzyme B expression (Fig. 7A). We then analyzed the correlation between PKCα expression and the abundance of infiltrating $CD8^+$ T cells *via* the TIMER database[51]. The results revealed that *PKCα* expression was positively correlated with $CD8^+$ T-cell infiltration in breast cancer patients, especially in those with luminal and basal subtypes (Supporting Information Fig. S8). Therefore, *PKCα*

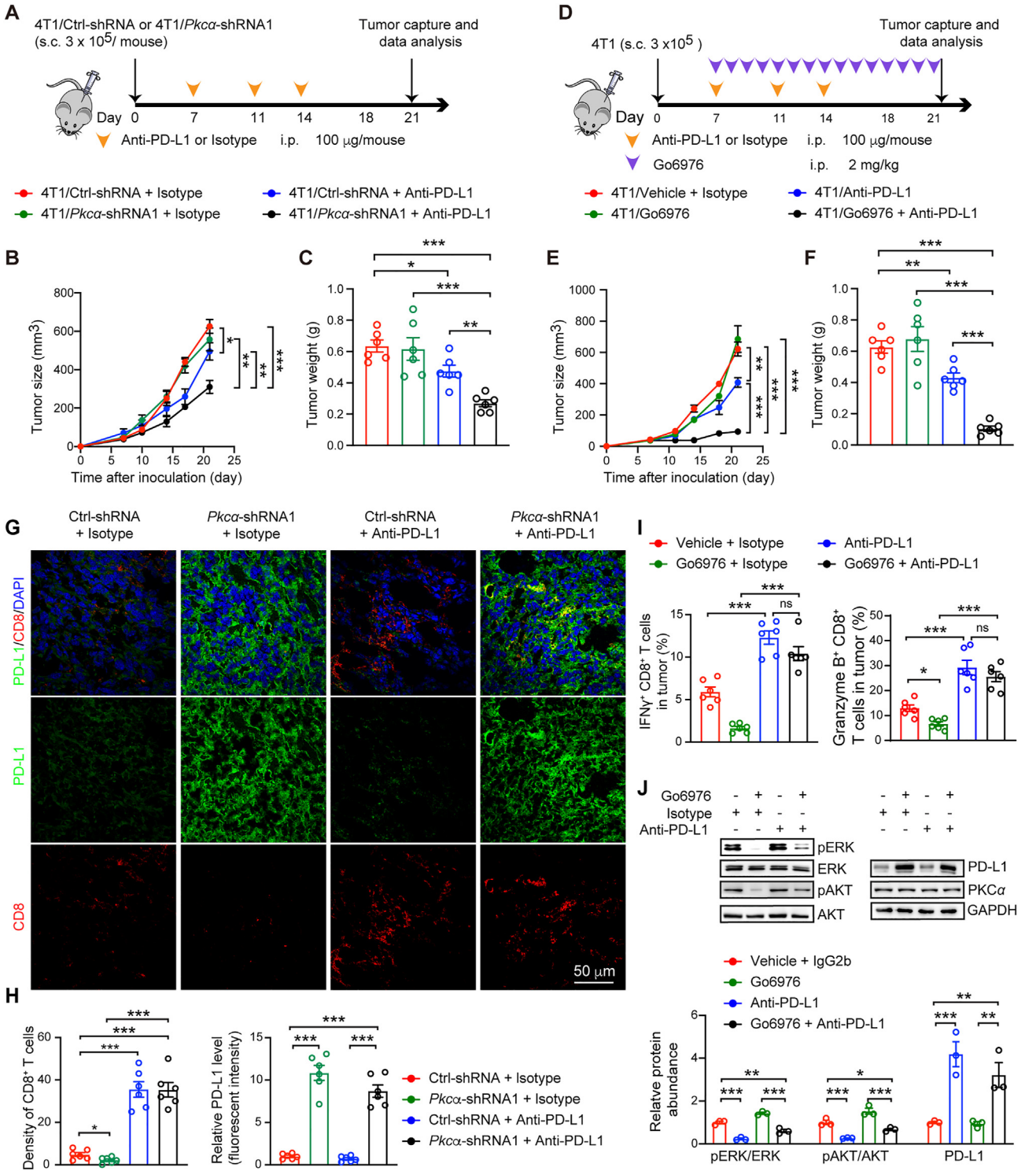

Figure 5 PKCα inhibition synergistically enhances anti-PD-L1 mAb activity in breast cancer cells. (A–C) BALB/c mice implanted with 4T1 cells transfected with either Ctrl-shRNA or *Pkca*-shRNA1 were treated with an anti-PD-L1 mAb or an IgG2b isotype control ($n = 6$). (A) A schematic view of the treatment plan. (B) Tumor volumes over time (days). (C) Weights of the tumors excised from each group. (D–F) Growth and weight of 4T1 tumors in female BALB/c mice after treatment with a single agent or in combination ($n = 6$). (D) A schematic view of the treatment plan. (E) Tumor volumes over time (days). (F) Weights of the tumors excised from each group. (G, H) The expression of PD-L1 and CD8α in allograft tumors from mice implanted with 4T1 cells transfected with either Ctrl-shRNA or *Pkcα*-shRNA1 was detected by immunofluorescence staining. Representative images with 50 μm scale bars (G) and statistical quantification (H) are shown. (I) Flow cytometric quantification of the percentages of IFNγ$^+$ CD8$^+$ cells (left) and granzyme B$^+$ CD8$^+$ cells (right) among CD8$^+$ T cells from allograft tumors derived from 4T1 tumor-bearing mice treated with a single agent or combination therapy. (J) IB (top) and quantitative analyses (bottom) of ERK and AKT signaling, PD-L1, and PKCα from 4T1 tumor-bearing mice treated with a single agent or combination therapy. The results are presented as the mean ± SEM. $^*P < 0.05$, $^{**}P < 0.01$, $^{***}P < 0.001$, ns means not significant.

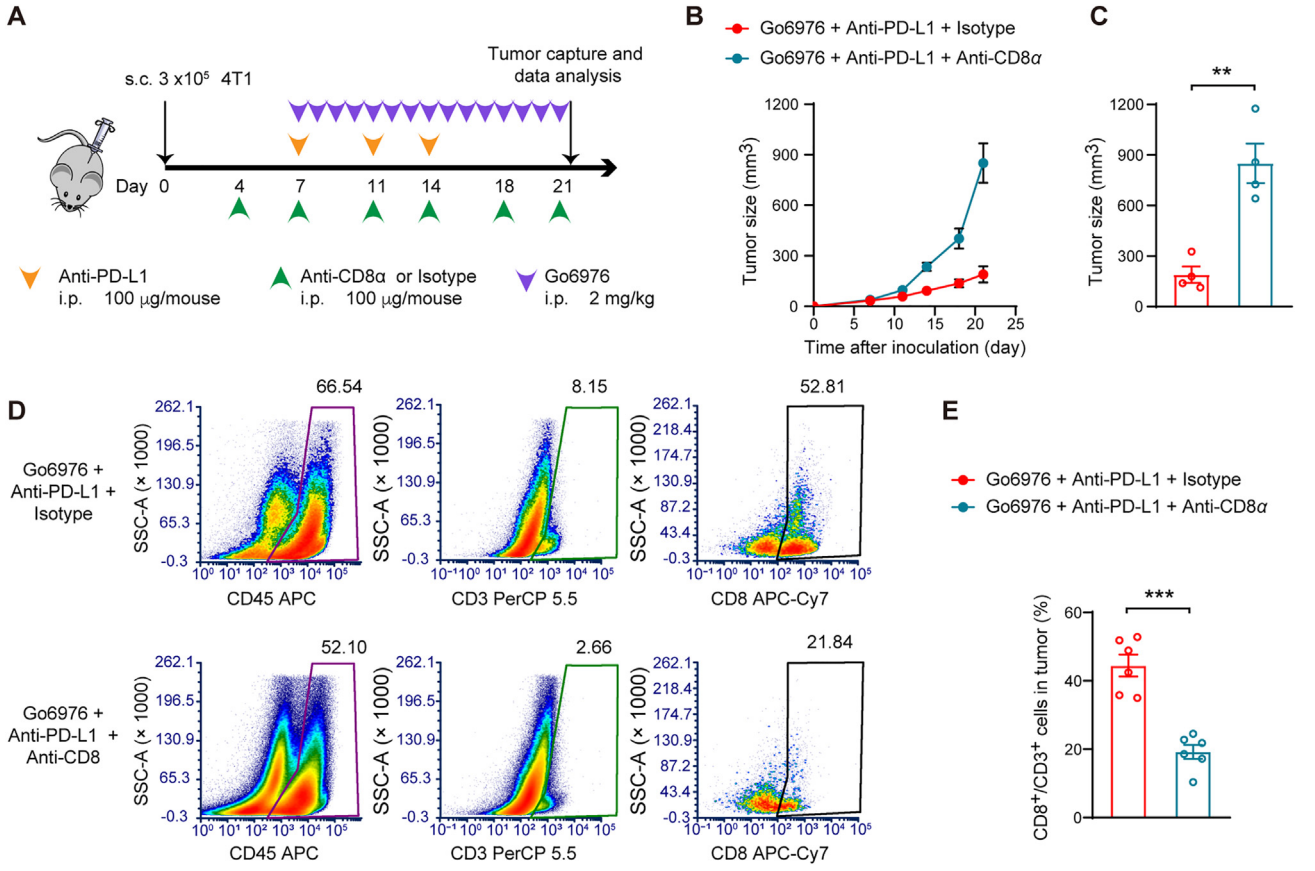

Figure 6 The synergistic effect of combination treatment comprising PKCα inhibition and an anti-PD-L1 mAb is dependent on CD8$^+$ T cells. Tumor growth and tumor weights of 4T1 cell allografts in female BALB/c mice after treatment with a single agent or combination of agents ($n = 6$). (A) A schematic view of the treatment plan. (B) Tumor volumes over time (days). (C) Volumes of the tumors excised from each group. (D, E) Flow cytometric assays (D) and quantification (E) of the CD8$^+$ population among CD3$^+$ TILs from allografted tumors. The results are presented as the mean ± SEM, $n = 6$; $^{**}P < 0.01$, $^{***}P < 0.001$.

expression is negatively correlated with PD-L1 expression and may contribute to CD8$^+$ T-cell potency in breast cancer.

Notably, several other tumor types, including lung cancer, colon cancer, and pancreatic cancer, exhibited similar immune effector gene pathway enrichment in tumor tissues with high PKCα expression (Fig. 7B), suggesting that the concept of PKCα inhibition accounting for the immunosuppressive phenotype may have broader relevance. Given that this positive correlation was also observed with several other PKC isozymes, such as PKCβ, PKCγ, PKCη, and PKCθ (Fig. 7B), we determined whether these PKC isozymes function as potential PD-L1 regulators. The results indicated that PKCβ and PKCθ negatively regulated PD-L1, while PKCγ and PKCη did not affect PD-L1 expression in MDA-MB-231 cells (Fig. 7C). However, treatment with the PKCβ selective inhibitor enzastaurin or the PKCθ inhibitor compound 20 did not enhance the antitumor effect of anti-PD-L1 mAb therapy (Fig. 7D). Moreover, there was no difference in activated CD8$^+$ T-cell infiltration among the vehicle-, enzastaurin- or compound 20-treated groups (Supporting Information Fig. S9A−S9C), suggesting that other factors also regulate the effect of PKCβ and PKCθ on antitumor immunity. Compared with PKCα, the expression of PKCβ and PKCθ was lower in most breast cancer cells (Fig. S9D−S9F). These results suggest that the therapeutic effects of PKCα inhibitors in combination with anti-PD-L1 mAb therapy may be intensified in breast cancer treatment.

In summary, our data demonstrate that PKCα has pleiotropic context-dependent functions in breast cancer. PKCα promotes cancer cell proliferation and survival through the ERK and AKT signaling axes. On the other hand, PKCα-mediated PD-L1 phosphorylation promotes PD-L1 degradation *via* β-TRCP, thereby enhancing antitumor immunity. Thus, combination therapy with anti-PD-L1 mAbs may be a more efficient clinical antitumor solution for PKCα-targeted therapy, especially for PKCα inhibitors (Fig. 7E).

4. Discussion

PKCα has been recognized as a critical tumor promoter for several decades, with a 9.46% amplification frequency in the TCGA invasive breast carcinoma dataset[52,53]. The drugging of catalytic kinase activity and noncatalytic scaffold domains still offers much promise, but how and when this occurs remain unclear[1,54]. Despite multiple efforts, including the use of the PKCα antisense nucleotide ISIS 3521 for lung cancer and breast cancer treatment, no PKCα-targeted therapy has been approved for the treatment of solid cancer, suggesting that a more comprehensive understanding of PKCα is needed[1,11,55,56]. The extent to which PKC activation or absence impacts the tumor microenvironment, especially the innate or adaptive immune system, is connected to defining its

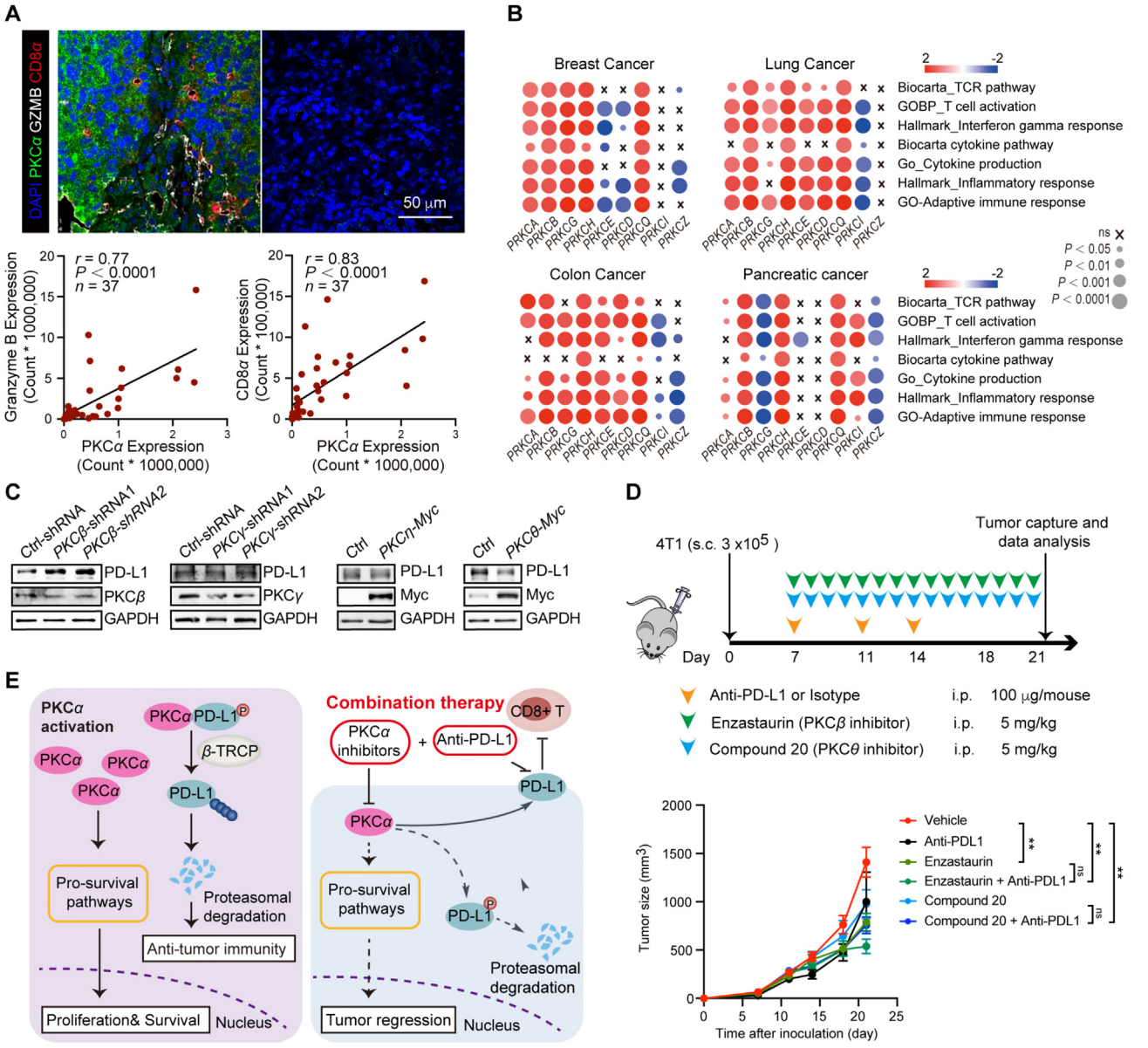

Figure 7 PKCα expression is correlated with immune gene signatures in cancer patients. (A) Representative microphotographs (top, scale bars, 50 μm) and correlation analyses (bottom) of multiplex immunofluorescence for PKCα (green), CD8α (red), and granzyme B (white) in primary breast tumor tissues. Each point represents the value of one patient. The *P* value was calculated by the Spearman correlation test. (B) GSEA demonstrating the correlation between PKC family members (bottom) and immune effector gene pathways (right panels) in cancer patients with four different cancer types. (C) IB analysis of the expression of PD-L1, PKCβ, PKCγ, and Myc in MDA-MB-231 cells transfected with the indicated shRNAs or overexpression plasmids, as shown at the top. (D) Growth of 4T1 tumors in female BALB/c mice after treatment with a single agent or combination of agents ($n = 6$). Upper: A schematic view of the treatment plan. Lower: Tumor volumes over time (days). (E) Schematic diagram illustrating the pleiotropic context-dependent functions of PKCα in cancer. (left) PKCα-mediated ERK and AKT signaling activation promotes cancer cell proliferation and survival. However, PKCα also phosphorylates PD-L1 and promotes PD-L1 degradation through β-TRCP, which contributes to antitumor immunity. (right) Immune checkpoint therapy, an anti-PD-L1 mAb, synergistically enhances the therapeutic effects of PKCα inhibitors, representing a potential therapeutic approach against breast cancer. $^{**}P < 0.01$, ns means not significant.

promotion and/or suppressor functions[1]. Here, we focused primarily on the effects of PKCα on TNBC, given that TNBC is a highly malignant, heterogeneous cancer with the worst outcome but is characterized by a high mutational load, which renders the tumor immunogenic and amenable to immunotherapeutic intervention compared with other types of breast cancer[26,57]. In this study, we demonstrated the connection between PKCα inhibition and tumor evasion from a protein quality control perspective. Inhibition of PKCα enhances $CD8^+$ T-cell-mediated tumor evasion and abolishes antitumor activity in immunocompetent mice. PKCα interacts with PD-L1, enhances PD-L1 phosphorylation, promotes PD-L1 degradation through β-TRCP, and

consequently suppresses PD-L1 expression. The therapeutic effects of PKCα inhibitors were intensified by synergizing with anti-PD-L1 mAb therapy to boost antitumor T-cell immunity *in vivo*. The anti-CD8α mAb blocked these synergistic effects in mice that received combination treatment with Go6976 and the anti-PD-L1 mAb. Our work indicates that interfering with the PKCα/PDL1 interaction may clarify the plasticity of PKCα in cancer treatment. Targeting PKCα in combination with anti-PD-L1 mAb therapy is a potential therapeutic approach for treating breast cancer, especially TNBC.

Recent studies have indicated that highly expressed PKCα in TNBC cells facilitates tumor growth and metastasis and maintains stemness[8,58-60]. Consistent with these findings, our *in vitro* and *in vivo* immunodeficient systems revealed that the activation of PKCα indeed triggers prosurvival pathways, such as the ERK and AKT pathways, and confers a tumor growth advantage in TNBC. However, its tumor-promoting function was weakened in an immunocompetent mouse model, implying that an intact immune system may impair the tumor-promoting function of PKCα. Furthermore, we revealed that PKCα negatively regulates PD-L1 *via* protein−protein interactions and plays a critical role in enhancing T-cell-dependent antitumor immunity. In this context, PKCα can be considered a tumor suppressor. Once PKCα is inhibited, the expression of PD-L1 is upregulated, and immune evasion occurs, which may explain the failure of PKC-targeted therapy. The tumor-suppressive role of PKCα has been supported in the $Apc^{Min/+}$ (multiple intestinal neoplasia) mouse model, KRAS-driven lung adenocarcinoma model, and hepatocellular carcinoma tumor model [61-63]. In addition to PKCα, several other PKC kinases, such as PKCβ and PKCζ, have been reported to exert versatile tumor-suppressive functions and are significantly mutated in cancer[2,64,65]. As targeting PKC may yield mixed results across different systems, the tissue- and/or cancer-specific role of PKC family members in tumor formation and progression needs to be re-explored in the future, especially when PKC-targeted therapy is considered.

According to the results of the present study, PKCα acts as a binding partner of PD-L1 and promotes PD-L1 phosphorylation. PKCα-mediated PD-L1 phosphorylation promotes PD-L1 degradation *via* β-TRCP, which enhances antitumor immunity. This PKCα/PD-L1 interaction provides new links between PD-L1 upregulation and PKCα inhibition from a protein quality control perspective. In addition to affecting PD-L1, PKCα may also affect the expression of other genes, contributing to the antitumor effects of PKCα. Evidence shows that PKCα negatively regulates β-catenin to inhibit colon cancer proliferation and suppress intestinal tumor formation in $Apc^{Min/+}$ mice[61,66]. Additionally, PKCα suppresses Kras-mediated lung tumor formation by activating the p38 MAPK-TGFβ signaling axis[62]. PKCα contributes to immune evasion in ZFP64-positive hepatocellular carcinoma cells by releasing CSF1[63]. In this study, we demonstrated, at least in breast cancer, that the antitumor role of PKCα is dependent on decreased PD-L1 expression and enhanced $CD8^+$ T-cell activity. Our results not only provide compelling evidence for a PKCα/β-TRCP/PD-L1 signaling axis that drives the tumor-suppressive effects of PKCα but also reveal an opportunity for future combinatory cancer therapies with anti-PD-1/PD-L1 mAbs.

Despite its high immunogenicity, TNBC immunotherapy is ineffective and requires combination therapy[25,67]. According to the IMpassion130 trial, the combination of atezolizumab with chemotherapy (nab-paclitaxel) is considered a standard therapy for PD-L1-positive metastatic TNBC[68,69]. Protein kinases are commonly exploited targets for cancer therapy[39,70,71]. Many kinase-targeting small molecules have been developed in the past 30 years. Small-molecule therapies offer many advantages, including low cost, good patient compliance, and easy access to intracellular targets[39]. The combination of small-molecule kinase inhibitors with anti-PD-1/PD-L1 antibodies provides attractive therapeutic strategies against many different cancers[38,72,73]. Here, our study showed that PD-L1 blockade restored antitumor immunity in PKCα-deficient breast tumors. The efficacy of PKCα inhibitors was intensified by synergizing with anti-PD-L1 mAb therapy to boost antitumor T-cell immunity *in vivo*. The combination of PKCα inhibitors and anti-PD-L1 antibodies led to significant tumor shrinkage in TNBC. These encouraging synergistic effects may contribute to the satisfactory efficacy of PKCα inhibitors in relevant clinical trials.

In the present study, the immunostimulatory activity of PKCα was validated mainly with Go6976, a selective PKCα kinase inhibitor. A critical issue that needs to be considered is its specificity, as it is challenging to generate truly isozyme-selective PKCα inhibitors. Some evidence has shown the pleiotropic context-dependent functions of PKC family members in controlling the immunosuppressive phenotype[2]. For example, in keeping with the notion that PKCα is essential for antitumor immunity, additional studies have shown that PKCζ loss impairs IFN and $CD8^+$ T-cell responses; simultaneous blockade of both PKCλ/ι and PKCζ in the intestinal epithelium impairs immunosurveillance and drives serrated intestinal cancer progression[74]. However, PKCι cooperates with YAP1 and PD-L1 to support the formation of an immunosuppressive microenvironment in ovarian and pancreatic cancer, respectively[75,76]. PKCλ/ι inactivation results in hyperstimulation of the ULK2-mediated IFN cascade, which represses the growth of intestinal tumors[77]. Moreover, PKCη and its CTLA-4 association in the Treg cell immunological synapses are required for Treg cell suppression[78]. According to our results covering several cancer types, although PKCα is positively correlated with antitumor immune signatures in patients, the correlations between antitumor immune signatures and other individual members of the PKC family seem not to be consistent. Several PKC family members were negative predictors of immune signatures in specific tumor types. Due to the high isozyme, tissue-specific, and plastic roles of PKCduring tumor progression, it is critical to develop potent and highly selective inhibitors for kinase targeting. However, this is still an ongoing challenge. Given the demonstrated synergistic effect of Go6976 and anti-PD-L1 antibody therapy in TNBC, we will determine whether our findings have far-reaching implications for other cancer types in the future. Additionally, it is necessary to address whether other PKC inhibitors enhance the efficacy of immunotherapy, which may provide new opportunities for cancer intervention. A systematic study will be required to understand the target biology and avoid complicating off-target effects.

In summary, our study indicated that PKCα interacts with and phosphorylates PD-L1, which contributes to PD-L1 degradation through β-TRCP. This PKCα/PD-L1 interaction reveals the tumor-suppressive role of PKCα, as PKCα inhibition abolishes antitumor activity in immunocompetent mice and enhances $CD8^+$ T-cell-mediated tumor evasion. Immune checkpoint blockade therapies overcome the disadvantages of PKCα inhibitors. Thus, this work provides a proof-of-concept for targeting PKCα in combination with anti-PD-L1 mAb therapy as a potential therapeutic approach against breast cancer, especially TNBC.

5. Conclusions

This study identified a unique role of PKCα in antitumor immunity. We found that PKCα inhibition suppressed breast cancer cell growth *in vitro* and *in vivo* in immune-deficient mice. However, this inhibition induces the upregulation of PD-L1 expression, which inactivates cocultured T cells *in vitro*, compromises antitumor immunity *in vivo*, and reduces antitumor efficacy in an immune-competent mouse model. Notably, PD-L1 mAb treatment enhances the efficacy of PKCα inhibition in an immune-competent mouse model. Mechanistically, we identified PKCα as a binding partner of PD-L1, and PKCα-mediated PD-L1 phosphorylation promoted PD-L1 degradation in a β-TRCP-dependent manner. Taken together, our study reveals a new molecular mechanism that regulates the stability of PD-L1. Moreover, combining pharmacological PKCα inhibitors with immune checkpoint blockade could be a potential therapeutic approach for enhancing the therapeutic efficacy of treatment for breast cancer, especially triple-negative breast cancer.

Acknowledgments

This work was supported by grants from the National Natural Science Foundation of China (82173853, 82173379, 82373914, 82073892), Chinese Academy of Medical Sciences (CAMS) Innovation Fund for Medical Sciences (2022-I2M-2-002, 2021-I2M-1−026 and 2021-I2M-1−016, China), CAMS Central Public-interest Scientific Institution Basal Research Fund (2018PT35004, China), Beijing Outstanding Young Scientist Program (BJJWZYJH01201910023028, China) and Peking Union Medical College Graduate Innovation Fund (2019-1007-05, China). We are grateful to Prof. Bo Huang's laboratory for providing 4T1 cells.

Author contributions

Jiaojiao Yu: Writing − review & editing, Writing − original draft, Visualization, Methodology, Investigation, Funding acquisition, Conceptualization. Yujin Xiang: Writing − original draft, Visualization, Methodology, Investigation, Funding acquisition. Yuzhen Gao: Methodology, Investigation. Shan Chang: Methodology. Ren Kong: Methodology. Xiaoxi Lv: Methodology. Jinmei Yu: Methodology. Yunjie Jin: Investigation. Chenxi Li: Investigation. Yiran Ma: Investigation. Zhenhe Wang: Investigation. Jichao Zhou: Investigation. Hongyu Yuan: Investigation. Shuang Shang: Investigation. Fang Hua: Investigation. Xiaowei Zhang: Investigation. Bing Cui: Writing − review & editing, Writing − original draft, Supervision, Funding acquisition, Conceptualization. Pingping Li: Writing − review & editing, Writing − original draft, Supervision, Funding acquisition, Conceptualization.

Conflicts of interest

The authors declare no conflicts of interest.

Appendix A. Supporting information

Supporting information to this article can be found online at https://doi.org/10.1016/j.apsb.2024.08.003.

References

1. Parker PJ, Brown SJ, Calleja V, Chakravarty P, Cobbaut M, Linch M, et al. Equivocal, explicit and emergent actions of PKC isoforms in cancer. *Nat Rev Cancer* 2021;**21**:51−63.
2. Reina-Campos M, Diaz-Meco MT, Moscat J. The dual roles of the atypical protein kinase Cs in cancer. *Cancer Cell* 2019;**36**:218−35.
3. Li SC, Cheng YT, Wang CY, Wu JY, Chen ZW, Wang JP, et al. *Actinobacillus pleuropneumoniae* exotoxin ApxI induces cell death *via* attenuation of FAK through LFA-1. *Sci Rep* 2021;**11**:1753.
4. Park SK, Hwang YS, Park KK, Park HJ, Seo JY, Chung WY. Kalopanaxsaponin A inhibits PMA-induced invasion by reducing matrix metalloproteinase-9 *via* PI3K/Akt- and PKCδ-mediated signaling in MCF-7 human breast cancer cells. *Carcinogenesis* 2009;**30**:1225−33.
5. Kawakami Y, Nishimoto H, Kitaura J, Maeda-Yamamoto M, Kato RM, Littman DR, et al. Protein kinase C βII regulates Akt phosphorylation on Ser-473 in a cell type- and stimulus-specific fashion. *J Biol Chem* 2004;**279**:47720−5.
6. Scerri J, Scerri C, Schafer-Ruoff F, Fink S, Templin M, Grech G. PKC-mediated phosphorylation and activation of the MEK/ERK pathway as a mechanism of acquired trastuzumab resistance in HER2-positive breast cancer. *Front Endocrinol* 2022;**13**:1010092.
7. Salama MF, Liu M, Clarke CJ, Espaillat MP, Haley JD, Jin T, et al. PKCα is required for Akt−mTORC1 activation in non-small cell lung carcinoma (NSCLC) with EGFR mutation. *Oncogene* 2019;**38**:7311−28.
8. Tam WL, Lu H, Buikhuisen J, Soh BS, Lim E, Reinhardt F, et al. Protein kinase C alpha is a central signaling node and therapeutic target for breast cancer stem cells. *Cancer Cell* 2013;**24**:347−64.
9. Lin W, Huang J, Yuan Z, Feng S, Xie Y, Ma W. Protein kinase C inhibitor chelerythrine selectively inhibits proliferation of triple-negative breast cancer cells. *Sci Rep* 2017;**7**:2022.
10. Lim PS, Sutton CR, Rao S. Protein kinase C in the immune system: from signalling to chromatin regulation. *Immunology* 2015;**146**:508−22.
11. Kawano T, Inokuchi J, Eto M, Murata M, Kang JH. Activators and inhibitors of protein kinase C (PKC): their applications in clinical trials. *Pharmaceutics* 2021;**13**:1748.
12. Isakov N. Protein kinase C (PKC) isoforms in cancer, tumor promotion and tumor suppression. *Semin Cancer Biol* 2018;**48**:36−52.
13. Newton AC. Protein kinase C as a tumor suppressor. *Semin Cancer Biol* 2018;**48**:18−26.
14. Cooke M, Magimaidas A, Casado-Medrano V, Kazanietz MG. Protein kinase C in cancer: the top five unanswered questions. *Mol Carcinog* 2017;**56**:1531−42.
15. Vinay DS, Ryan EP, Pawelec G, Talib WH, Stagg J, Elkord E, et al. Immune evasion in cancer: mechanistic basis and therapeutic strategies. *Semin Cancer Biol* 2015;**35**(Suppl):S185−98.
16. Hanahan D. Hallmarks of cancer: new dimensions. *Cancer Discov* 2022;**12**:31−46.
17. Binnewies M, Roberts EW, Kersten K, Chan V, Fearon DF, Merad M, et al. Understanding the tumor immune microenvironment (TIME) for effective therapy. *Nat Med* 2018;**24**:541−50.
18. Xiao Q, Li X, Liu C, Jiang Y, He Y, Zhang W, et al. Improving cancer immunotherapy *via* co-delivering checkpoint blockade and thrombospondin-1 downregulator. *Acta Pharm Sin B* 2023;**13**:3503−17.
19. Sukari A, Nagasaka M, Al-Hadidi A, Lum LG. Cancer immunology and immunotherapy. *Anticancer Res* 2016;**36**:5593−606.
20. Andrews LP, Yano H, Vignali DAA. Inhibitory receptors and ligands beyond PD-1, PD-L1 and CTLA-4: breakthroughs or backups. *Nat Immunol* 2019;**20**:1425−34.
21. Wang F, Fu K, Wang Y, Pan C, Wang X, Liu Z, et al. Small-molecule agents for cancer immunotherapy. *Acta Pharm Sin B* 2024;**14**:905−52.
22. Morad G, Helmink BA, Sharma P, Wargo JA. Hallmarks of response, resistance, and toxicity to immune checkpoint blockade. *Cell* 2021;**184**:5309−37.

23. Adams S, Gatti-Mays ME, Kalinsky K, Korde LA, Sharon E, Amiri-Kordestani L, et al. Current landscape of immunotherapy in breast cancer: a review. *JAMA Oncol* 2019;**5**:1205−14.
24. Bassez A, Vos H, Van Dyck L, Floris G, Arijs I, Desmedt C, et al. A single-cell map of intratumoral changes during anti-PD1 treatment of patients with breast cancer. *Nat Med* 2021;**27**:820−32.
25. Bianchini G, De Angelis C, Licata L, Gianni L. Treatment landscape of triple-negative breast cancer—expanded options, evolving needs. *Nat Rev Clin Oncol* 2022;**19**:91−113.
26. Michel LL, von Au A, Mavratzas A, Smetanay K, Schutz F, Schneeweiss A. Immune checkpoint blockade in patients with triple-negative breast cancer. *Target Oncol* 2020;**15**:415−28.
27. Zheng M, Zhang W, Chen X, Guo H, Wu H, Xu Y, et al. The impact of lipids on the cancer-immunity cycle and strategies for modulating lipid metabolism to improve cancer immunotherapy. *Acta Pharm Sin B* 2023;**13**:1488−97.
28. Zou W, Wolchok JD, Chen L. PD-L1 (B7-H1) and PD-1 pathway blockade for cancer therapy: mechanisms, response biomarkers, and combinations. *Sci Transl Med* 2016;**8**:328rv4.
29. Doroshow DB, Bhalla S, Beasley MB, Sholl LM, Kerr KM, Gnjatic S, et al. PD-L1 as a biomarker of response to immune-checkpoint inhibitors. *Nat Rev Clin Oncol* 2021;**18**:345−62.
30. Chen J, Jiang CC, Jin L, Zhang XD. Regulation of PD-L1: a novel role of pro-survival signalling in cancer. *Ann Oncol* 2016;**27**:409−16.
31. Krueger J, Rudd CE, Taylor A. Glycogen synthase 3 (GSK-3) regulation of PD-1 expression and and its therapeutic implications. *Semin Immunol* 2019;**42**:101295.
32. Fan Z, Wu C, Chen M, Jiang Y, Wu Y, Mao R, et al. The generation of PD-L1 and PD-L2 in cancer cells: from nuclear chromatin reorganization to extracellular presentation. *Acta Pharm Sin B* 2022;**12**:1041−53.
33. Li CW, Lim SO, Xia W, Lee HH, Chan LC, Kuo CW, et al. Glycosylation and stabilization of programmed death ligand-1 suppresses T-cell activity. *Nat Commun* 2016;**7**:12632.
34. Chan LC, Li CW, Xia W, Hsu JM, Lee HH, Cha JH, et al. IL-6/JAK1 pathway drives PD-L1 Y112 phosphorylation to promote cancer immune evasion. *J Clin Invest* 2019;**129**:3324−38.
35. Cha JH, Yang WH, Xia W, Wei Y, Chan LC, Lim SO, et al. Metformin promotes antitumor immunity *via* endoplasmic-reticulum-associated degradation of PD-L1. *Mol Cell* 2018;**71**:606−20.e7.
36. Dai X, Bu X, Gao Y, Guo J, Hu J, Jiang C, et al. Energy status dictates PD-L1 protein abundance and anti-tumor immunity to enable checkpoint blockade. *Mol Cell* 2021;**81**:2317−331.e6.
37. Zhang J, Bu X, Wang H, Zhu Y, Geng Y, Nihira NT, et al. Cyclin D-CDK4 kinase destabilizes PD-L1 *via* cullin 3-SPOP to control cancer immune surveillance. *Nature* 2018;**553**:91−5.
38. Li H, Li CW, Li X, Ding Q, Guo L, Liu S, et al. MET inhibitors promote liver tumor evasion of the immune response by stabilizing PDL1. *Gastroenterology* 2019;**156**:1849−61.e13.
39. Ferguson FM, Gray NS. Kinase inhibitors: the road ahead. *Nat Rev Drug Discov* 2018;**17**:353−77.
40. Kilkenny C, Browne W, Cuthill IC, Emerson M, Altman DG, Group NCRRGW. Animal research: reporting *in vivo* experiments: the ARRIVE guidelines. *Br J Pharmacol* 2010;**160**:1577−9.
41. Butcher EC, Berg EL, Kunkel EJ. Systems biology in drug discovery. *Nat Biotechnol* 2004;**22**:1253−9.
42. Suhail Y, Cain MP, Vanaja K, Kurywchak PA, Levchenko A, Kalluri R, et al. Systems biology of cancer metastasis. *Cell Syst* 2019;**9**:109−27.
43. Li Rui, Guo Xiuping, Han Yanxing, Wang Lulu, Jiang Jiandong. The biological principle of biao Ben Jian Zhi. *Acta Pharm Sin* 2023;**58**:351−9.
44. Cao Z, Liao Q, Su M, Huang K, Jin J, Cao D. AKT and ERK dual inhibitors: the way forward?. *Cancer Lett* 2019;**459**:30−40.
45. Li W, Zhang J, Flechner L, Hyun T, Yam A, Franke TF, et al. Protein kinase C-alpha overexpression stimulates Akt activity and suppresses apoptosis induced by interleukin 3 withdrawal. *Oncogene* 1999;**18**:6564−72.
46. Li D, Shatos MA, Hodges RR, Dartt DA. Role of PKCα activation of Src, PI-3K/AKT, and ERK in EGF-stimulated proliferation of rat and human conjunctival goblet cells. *Invest Ophthalmol Vis Sci* 2013;**54**:5661−74.
47. Liu H, Kuang X, Zhang Y, Ye Y, Li J, Liang L, et al. ADORA1 inhibition promotes tumor immune evasion by regulating the ATF3−PD-L1 Axis. *Cancer Cell* 2020;**37**:324−39.e8.
48. Zhou J, Kryczek I, Li S, Li X, Aguilar A, Wei S, et al. The ubiquitin ligase MDM2 sustains STAT5 stability to control T cell-mediated antitumor immunity. *Nat Immunol* 2021;**22**:460−70.
49. Sen T, Rodriguez BL, Chen L, Corte CMD, Morikawa N, Fujimoto J, et al. Targeting DNA damage response promotes antitumor immunity through STING-mediated T-cell activation in small cell lung cancer. *Cancer Discov* 2019;**9**:646−61.
50. Yang Y, Li CW, Chan LC, Wei Y, Hsu JM, Xia W, et al. Exosomal PD-L1 harbors active defense function to suppress T cell killing of breast cancer cells and promote tumor growth. *Cell Res* 2018;**28**:862−4.
51. Li T, Fu J, Zeng Z, Cohen D, Li J, Chen Q, et al. TIMER2.0 for analysis of tumor-infiltrating immune cells. *Nucleic Acids Res* 2020;**48**:W509−14.
52. Castagna M, Takai Y, Kaibuchi K, Sano K, Kikkawa U, Nishizuka Y. Direct activation of calcium-activated, phospholipid-dependent protein kinase by tumor-promoting phorbol esters. *J Biol Chem* 1982;**257**:7847−51.
53. Cerami E, Gao J, Dogrusoz U, Gross BE, Sumer SO, Aksoy BA, et al. The cBio cancer genomics portal: an open platform for exploring multidimensional cancer genomics data. *Cancer Discov* 2012;**2**:401−4.
54. Wang Z, Huang W, Zhou K, Ren X, Ding K. Targeting the non-catalytic functions: a new paradigm for kinase drug discovery?. *J Med Chem* 2022;**65**:1735−48.
55. Mackay HJ, Twelves CJ. Targeting the protein kinase C family: are we there yet?. *Nat Rev Cancer* 2007;**7**:554−62.
56. Tortora G, Ciardiello F. Antisense strategies targeting protein kinase C: preclinical and clinical development. *Semin Oncol* 2003;**30**:26−31.
57. Yu JM, Sun W, Wang ZH, Liang X, Hua F, Li K, et al. TRIB3 supports breast cancer stemness by suppressing FOXO1 degradation and enhancing SOX2 transcription. *Nat Commun* 2019;**10**:5720.
58. Tonetti DA, Gao W, Escarzaga D, Walters K, Szafran A, Coon JS. PKCα and ERβ are associated with triple-negative breast cancers in African American and Caucasian patients. *Int J Breast Cancer* 2012;**2012**:740353.
59. Yue CH, Liu LC, Kao ES, Lin H, Hsu LS, Hsu CW, et al. Protein kinase C α is involved in the regulation of AXL receptor tyrosine kinase expression in triple-negative breast cancer cells. *Mol Med Rep* 2016;**14**:1636−42.
60. Pham TND, Perez White BE, Zhao H, Mortazavi F, Tonetti DA. Protein kinase C α enhances migration of breast cancer cells through FOXC2-mediated repression of p120-catenin. *BMC Cancer* 2017;**17**:832.
61. Oster H, Leitges M. Protein kinase C α but not PKCζ suppresses intestinal tumor formation in $Apc^{Min/+}$ mice. *Cancer Res* 2006;**66**:6955−63.
62. Hill KS, Erdogan E, Khoor A, Walsh MP, Leitges M, Murray NR, et al. Protein kinase Cα suppresses Kras-mediated lung tumor formation through activation of a p38 MAPK−TGFβ signaling axis. *Oncogene* 2014;**33**:2134−44.
63. Wei CY, Zhu MX, Zhang PF, Huang XY, Wan JK, Yao XZ, et al. PKCα/ZFP64/CSF1 axis resets the tumor microenvironment and fuels anti-PD1 resistance in hepatocellular carcinoma. *J Hepatol* 2022;**77**:163−76.
64. Antal CE, Hudson AM, Kang E, Zanca C, Wirth C, Stephenson NL, et al. Cancer-associated protein kinase C mutations reveal kinase's role as tumor suppressor. *Cell* 2015;**160**:489−502.
65. Galvez AS, Duran A, Linares JF, Pathrose P, Castilla EA, Abu-Baker S, et al. Protein kinase Cζ represses the interleukin-6 promoter and impairs tumorigenesis *in vivo*. *Mol Cell Biol* 2009;**29**:104−15.
66. Gwak J, Jung SJ, Kang DI, Kim EY, Kim DE, Chung YH, et al. Stimulation of protein kinase C-α suppresses colon cancer cell proliferation by down-regulation of β-catenin. *J Cell Mol Med* 2009;**13**:2171−80.

67. Li C, Lang J, Wang Y, Cheng Z, Zu M, Li F, et al. Self-assembly of CXCR4 antagonist peptide-docetaxel conjugates for breast tumor multi-organ metastasis inhibition. *Acta Pharm Sin B* 2023;**13**:3849−61.
68. Schmid P, Adams S, Rugo HS, Schneeweiss A, Barrios CH, Iwata H, et al. Atezolizumab and Nab-paclitaxel in advanced triple-negative breast cancer. *N Engl J Med* 2018;**379**:2108−21.
69. Emens LA. Immunotherapy in triple-negative breast cancer. *Cancer J* 2021;**27**:59−66.
70. Yu JJ, Zhou DD, Yang XX, Cui B, Tan FW, Wang J, et al. TRIB3−EGFR interaction promotes lung cancer progression and defines a therapeutic target. *Nat Commun* 2020;**11**:3660.
71. Wang F, Li Y, Yang Z, Cao W, Liu Y, Zhao L, et al. Targeting IL-17A enhances imatinib efficacy in Philadelphia chromosome-positive B-cell acute lymphoblastic leukemia. *Nat Commun* 2024;**15**:203.
72. Ebert PJR, Cheung J, Yang Y, McNamara E, Hong R, Moskalenko M, et al. MAP kinase inhibition promotes T cell and anti-tumor activity in combination with PD-L1 checkpoint blockade. *Immunity* 2016;**44**:609−21.
73. Deng J, Wang ES, Jenkins RW, Li S, Dries R, Yates K, et al. CDK4/6 inhibition augments antitumor immunity by enhancing T-cell activation. *Cancer Discov* 2018;**8**:216−33.
74. Nakanishi Y, Duran A, L'Hermitte A, Shelton PM, Nakanishi N, Reina-Campos M, et al. Simultaneous loss of both atypical protein kinase C genes in the intestinal epithelium drives serrated intestinal cancer by impairing immunosurveillance. *Immunity* 2018;**49**:1132−47.e7.
75. Sarkar S, Bristow CA, Dey P, Rai K, Perets R, Ramirez-Cardenas A, et al. PRKCI promotes immune suppression in ovarian cancer. *Genes Dev* 2017;**31**:1109−21.
76. Zhang H, Zhu Y, Wang J, Weng S, Zuo F, Li C, et al. PKCiota regulates the expression of PDL1 through multiple pathways to modulate immune suppression of pancreatic cancer cells. *Cell Signal* 2021;**86**:110115.
77. Linares JF, Zhang X, Martinez-Ordonez A, Duran A, Kinoshita H, Kasashima H, et al. PKClambda/iota inhibition activates an ULK2-mediated interferon response to repress tumorigenesis. *Mol Cell* 2021;**81**:4509−26.e10.
78. Kong KF, Fu G, Zhang Y, Yokosuka T, Casas J, Canonigo-Balancio AJ, et al. Protein kinase C-eta controls CTLA-4-mediated regulatory T cell function. *Nat Immunol* 2014;**15**:465−72.